DESIGN FOR ADDITIVE MANUFACTURING OF AUTOMOTIVE COMPONENTS VIA TOPOLOGY OPTIMIZATION

2022
MASTER THESIS
MECHANICAL ENGINEERING

Hüseyin BOTSALI

Assist.Prof.Dr. Cevat ÖZARPA

DESIGN FOR ADDITIVE MANUFACTURING OF AUTOMOTIVE COMPONENTS VIA TOPOLOGY OPTIMIZATION

Hüseyin BOTSALI

T.C.
Karabuk University
Institute of Graduate Programs
Department of Mechanical Engineering
Prepared as
Master Thesis

Assist.Prof.Dr. Cevat ÖZARPA

KARABUK
March 2022

I certify that in my opinion the thesis submitted by Hüseyin BOTSALI titled "DESIGN FOR ADDITIVE MANUFACTURING OF AUTOMOTIVE COMPONENTS VIA TOPOLOGY OPTIMIZATION" is fully adequate in scope and in quality as a thesis for the degree of Master of Science.

Assist.Prof.Dr. Cevat ÖZARPA .....
Thesis Advisor, Department of Mechanical Engineering

This thesis is accepted by the examining committee with a unanimous vote in the Department of Mechanical Engineering as a Master of Science thesis. Mar 7, 2022

Examining Committee Members (Institutions)	Signature
Chairman : Assoc.Prof.Dr. İsmail ESEN (KBU)	.....
Member : Assist.Prof.Dr. Cevat ÖZARPA (KBU)	.....
Member : Assist.Prof.Dr. Barkın BAKIR (MU)	.....

The degree of Master of Science by the thesis submitted is approved by the Administrative Board of the Institute of Graduate Programs, Karabuk University.

Prof. Dr. Hasan SOLMAZ .....
Director of the Institute of Graduate Programs

"I declare that all the information within this thesis has been gathered and presented in accordance with academic regulations and ethical principles and I have according to the requirements of these regulations and principles cited all those which do not originate in this work as well."

Hüseyin BOTSALI

ABSTRACT

M. Sc. Thesis

DESIGN FOR ADDITIVE MANUFACTURING OF AUTOMOTIVE COMPONENTS VIA TOPOLOGY OPTIMIZATION

Hüseyin BOTSALI

Karabük University
Institute of Graduate Programs
The Department of Mechanical Engineering

Thesis Advisor:
Assist. Prof. Dr. Cevat ÖZARPA
March 2022, 57 pages

The automotive industry, where studies are carried out in the field of motor vehicles, is developing day by day. Since it is an industry that is open to development, it is also open to innovations brought by additive manufacturing. With the design for additive manufacturing, components are replaced by new ones designed by removing production restrictions. These new models are generally lighter and more durable than the old ones.

Topology optimization has become a key element of design for additive manufacturing as it can enhance mechanical properties while reducing mass. In this study, the lower control arm of the double wishbone suspension system was taken as a model and topology optimization studies were carried out on the model. Finite element analyses were applied on the initial model and on the final model that emerged as a result of topology studies. Although stress, displacement and natural

frequencies remained almost constant in the optimized model, a mass reduction of %16,39 was achieved.

Key Words : Design for additive manufacturing, topology optimization, finite element analysis, powder bed fusion, suspension system.

Science Code : 91433

ÖZET

Yüksek Lisans Tezi

OTOMOTİV KOMPONENTLERİNİN TOPOLOJİ OPTİMİZASYONU İLE EKLEMELİ İMALAT İÇİN TASARIMI

Hüseyin BOTSALI

Karabük Üniversitesi
Lisansüstü Eğitim Enstitüsü
Makine Mühendisliği Anabilim Dalı

Tez Danışmanı:
Dr. Öğr. Üy. Cevat ÖZARPA
Mart 2022, 57 sayfa

Motorlu taşıtlar alanında çalışmaların gerçekleştirildiği otomotiv endüstrisi her geçen gün gelişmektedir. Gelişime açık bir endüstri olması nedeniyle eklemeli imalatın getirdiği yeniliklere de açıktır. Eklemeli imalat için tasarım ile komponentlerin yerini üretim kısıtlamaları kaldırılarak tasarlanan yenileri almaktadır. Bu yeni modeller eskilerine göre genellikle daha hafif ve daha dayanıklı olmaktadır.

Topoloji optimizasyonu, kütleyi hafifletirken mekanik özellikleri iyileştirebildiği için eklemeli imalat için tasarımın ana unsurlarından biri haline gelmiştir. Bu çalışmada çift salıncaklı süspansiyon sisteminin alt kontrol kolu örnek model alınmış ve topoloji optimizasyonu çalışmaları bu model üzerinde gerçekleştirilmiştir. Başlangıç modeli ve topoloji çalışmaları sonucu ortaya çıkan nihai model üzerinde sonlu elemanlar analizleri uygulanmıştır. Optimize edilmiş modelde gerilme, yer

değiştirme ve doğal frekansların neredeyse sabit kalmasına karşın, %16,39 kütlesel hafifleme sağlanmıştır.

Anahtar Kelimeler : Eklemeli imalat için tasarım, topoloji optimizasyonu, sonlu elemanlar analizi, toz yatağı füzyonu, süspansiyon sistemi.

Bilim Kodu **:** 91433

ACKNOWLEDGMENT

First of all, I would like to give thanks to my advisor, Assist. Prof. Dr. Cevat ÖZARPA, for his great interest and assistance in preparation of this thesis. I also thank to Bahadır Furkan KINACI for his support and contribution during the process of this thesis.

CONTENTS

Page

Page

Page

LIST OF FIGURES

Page

Page

LIST OF TABLES

Page

SYMBOLS AND ABBREVITIONS INDEX

SYMBOLS

ρ : density

σ : stress

σ_{vm} : von mises stress

ε : strain

u : displacement

ABBREVITIONS

DFAM : Design for Additive Manufacturing

A-Arm : Lower Control Arm

AM : Additive Manufacturing

L-PBF : Laser Powder Bed Fusion

FEM : Finite Element Method

FEA : Finite Element Analysis

SIMP : Solid Isotropic Material Penalization

F : Force

N : Newton

E : Young's Modulus

K : Stiffness Matrix

FWR : Front Weight Ratio

DOF : Degree of Freedom

PART 1

INTRODUCTION

The automotive industry is the sector in which studies on motor vehicles are carried out. Equipment produced in this industry is called automotive components. An automotive product consists of many components. To improve on a motor vehicle, it may be enough to make any of its components more efficient. Therefore, all automotive components are products of research and development.

Until recently, traditional manufacturing methods were generally used in the production of automotive components. With the spread of additive manufacturing technologies, changes began to occur in this situation. With the use of AM in the production of automotive components, most of the manufacturing constraints are eliminated and more independent production can be achieved.

Thanks to AM's elimination of the requirements of traditional manufacturing, it has become possible to make designs that are mechanically and massively superior to their previous designs. This has made substantial to design for additive manufacturing. The redesign and production of automotive components according to DFAM, within the scope of research and development activities, both brought great innovations to the automotive industry and brought excitement to the sector that opened the horizon for new studies.

The realization and production of DFAM on all automotive components is of great importance in the competitive industry. Topology optimization has become a prominent issue in these studies. Giving the optimum model that provides user with the desired mechanical and mass values makes him stand out in studies on DFAM. Topology optimization studies can be done within finite element softwares.

In this thesis, the design for additive manufacturing of automotive components is dealt with using topology optimization. While developing the methodology, the front lower control arm, which is an automotive component, was taken as the case study. As a result of the study, the model obtained from the optimization studies was compared with the first model and the ensuring improvements were revealed.

PART 2

LITERATURE REVIEW

In this thesis, a design for additive manufacturing was carried out by performing topology optimization on the suspension control arm, which is an automotive component. Topology optimization studies were applied with various goal and constraint strategies to observe different results. For this reason, the literature review was handled from three aspects before it was put into practice. These; design for additive manufacturing studies, multi-objective topology optimization studies, and suspension control arm topology optimization studies.

Mhapsekar et al. [1] developed two new DFAM constraints to enable additive manufacturing and topology optimization to work together efficiently. Reddy K. et al. [2] redesigned the steering knuckle in the student race car according to the DFAM criteria and achieved a significant mass gain. Ranjan et al. [3] developed two new design methodologies for DFAM and presented case studies on them. Tyflopoulos et al. [4] performed DFAM of brake caliper using topology optimization.

Lian et al. [5] developed a combined method using shape and topology optimizations, which are types of structural optimization, and showed that they can reduce stress while restricting the volume with this method. Lu et al. [6] conducted a mass reduction study of an electric vehicle's battery enclosure with topology optimization, taking into account both the static strength and dynamic frequencies. Dalklint et al. [7] developed a topology optimization method that minimizes artificial buckling modes while minimizing displacement with volume constraints.

Kulkarni et al. [8] carried out a study to lighten the mass with topology optimization for two different materials on the lower wishbone. Song et al. [9] implemented topology optimization on the upper control arm, taking into account the strength values. Viqaruddin et al. [10] obtained 30% lightness by maintaining their strength values in the lower control arm of the formula sae vehicle. Lin et al. [11] applied topology and size optimizations to the lower control arm based on the kinematic envelope technique.

A research article was published within the scope of studies to support the work done in the thesis and to prove the academic value of the study [12]. In this study, a topology optimization application was carried out on the draw hook used in rail vehicles. The results were not found satisfactory enough to transfer the body, which can be considered large for production with additive manufacturing, to the new production process.

PART 3

THEORETICAL BACKGROUND

The study has been theoretically examined under three main headings. These are automotive components, additive manufacturing and computer aided engineering. Automotive components are detailed with suspension system, which is the component studied. Powder bed fusion, which is frequently preferred in metal component production, is examined as an additive manufacturing method. In the section of CAE, finite element analysis and topology optimization are included.

3.1. AUTOMOTIVE COMPONENTS

An automobile consists of various systems such as engine, transmission, axle, suspension and brake. Each of these systems, individually and together, fulfills vital tasks. Each system is formed by the combination of certain parts. These parts are called automotive components. In the applications carried out in this thesis, the lower control arm of the front suspension system has been studied.

3.1.1. Suspension Systems

There are many parameters that express the power of a car. However, no matter how high these parameters are, the power must be controlled in order to get real performance from the car. Therefore, the suspension system is one of the most important automotive components. The suspension system, which provides the connection between the chassis and the wheels, performs very important control functions in terms of vehicle dynamics. The main control functions of the suspension system are as follows [13];

- It ensures convenient driving comfort.
- It provides road holding while driving, cornering and braking.
- It maintains the balance of the vehicle on uneven roads.
- It absorbs vibrations caused by imperfections in the road.
- It minimizes the damage caused by road defects to vehicle components.

Different types of suspension systems are used according to the application area. The most frequently used ones are shown in Figure 3.1. These are multipurpose suspension systems such as double wishbone, MacPherson and multilink, and solid suspension systems such as leaf springs and rigid links [14].

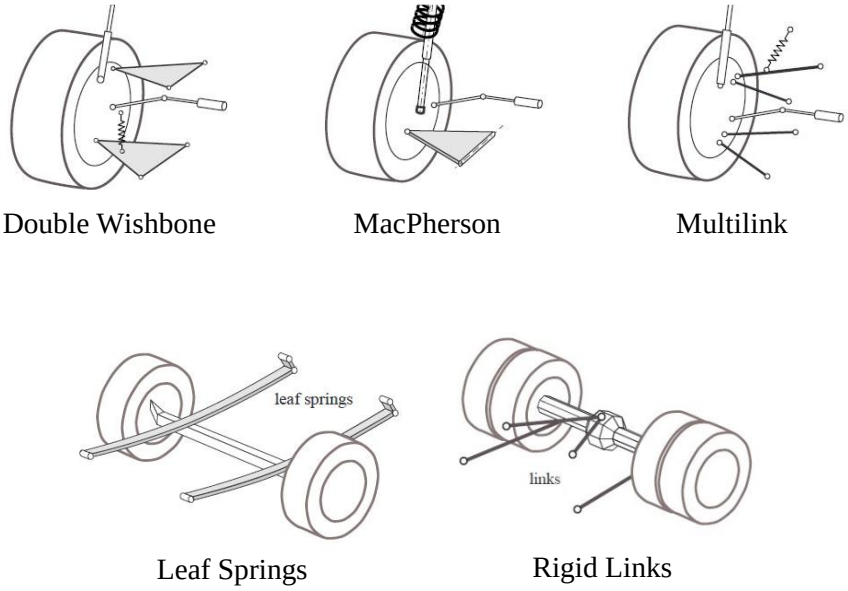

Figure 3.1. Various types of suspension systems.

3.1.2. Double Wishbone Suspension System

Different types of suspension systems can be preferred on the front and rear axle of the vehicle. The suspension system is examined in two main categories as dependent and independent. What makes this difference is whether the system allows the wheels to move independently of each other. Dependent suspension is mostly preferred on the rear axle or the front axle of truck-type vehicles. On the other hand, the independent suspension system has been the most widely used method for the

front wheels of cars since its inception. Two main methods are used as the independent front suspension system. These are the MacPherson and Double Wishbone methods shown in figure 3.2.

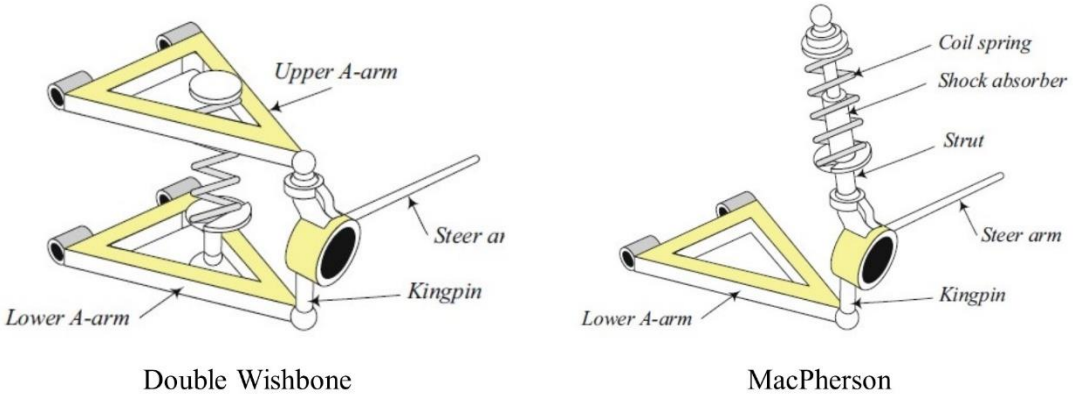

Figure 3.2. The double wishbone and MacPherson suspension systems.

In general, the Double Wishbone system has a design that provides the wheel connection with the two control arms and includes a shock absorber and a coil spring to dampen vibrations and shocks between these arms. Although it is larger and heavier than the MacPherson system, it is widely used on the front wheels of pickup-style large cars because it provides more steering and angular mobility [15].

3.1.2.1. Front Lower Control Arm

The lower control arm supports the entire front weight of the vehicle as well as controls front wheel movement. For this reason, it can be considered as the most important component of the front suspension system, even though it is part of the team that works together. The suspension system ensures that the tire moves in harmony with the shape of the road with the great effect of the lower control arm. In this way, both the handling of the vehicle increases and the loads on the chassis due to imperfect roads are minimized. It is crucial that the lower control arm, which performs such critical functions throughout the ride, can provide adequate performance. Therefore, parameters such as impact strength and natural frequencies should not be ignored while making new designs [16].

3.2. ADDITIVE MANUFACTURING

3.2.1. Description and History

Additive Manufacturing (AM) was invented in the late 1980s and has been used as rapid prototyping until the last 10 years. However, in the last 10 years, many researches and studies have been conducted for its use in industrial manufacturing. In this process, it has developed very rapidly and has become a method used by the largest production sectors to produce the most important components. With the method that emerged initially to manufacture prototypes from polymer materials, today pure metals, metal alloys and even metal matrix composites can be produced [17]. In Figure 3.3, the increase in the number of publications related to AM over the years can be observed [18].

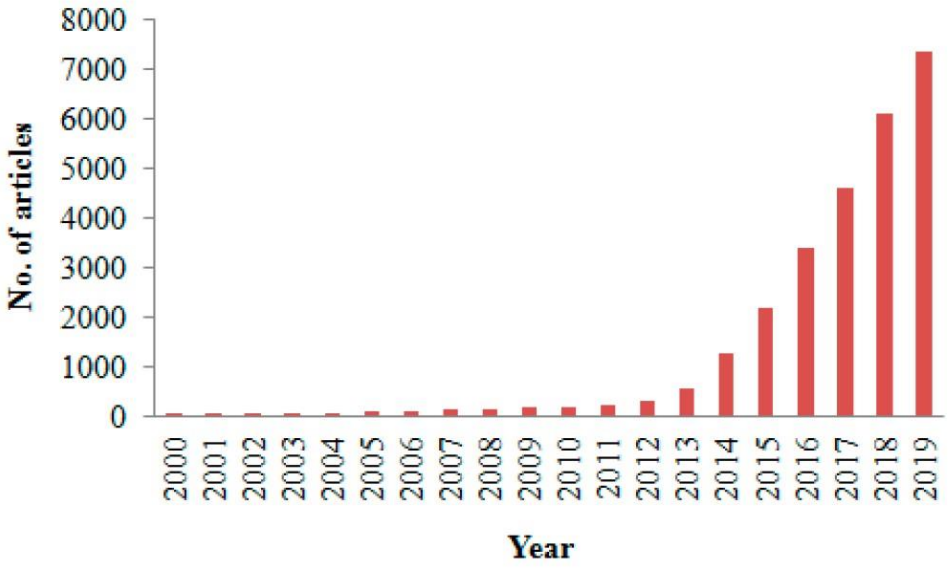

Figure 3.3. Number of publications related to AM according to years.

As seen in Figure 3.4, the AM industry has grown by more than 25% each year over the past ten years. This increase rate has decreased relatively in 2020 due to the covid19 pandemic. Despite this, the total revenues of AM system manufacturers from the sale of products and equipment to service providers increased by around 7% compared to the previous year and exceeded 5 billion dollars [19].

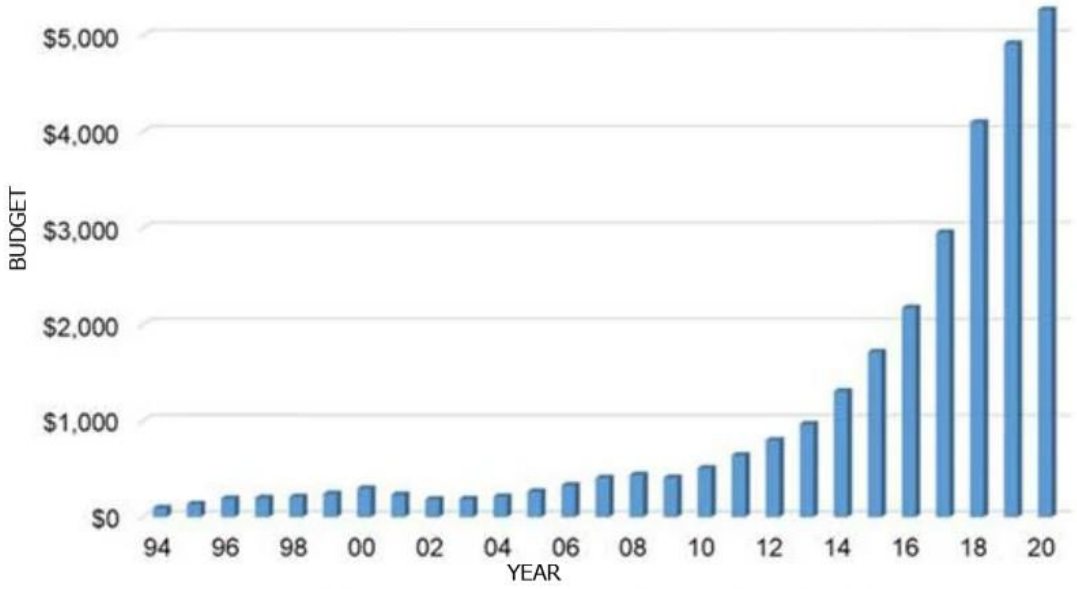

Figure 3.4. Production of AM parts by years.

The AM method brings an understanding which is the opposite of traditionally used methods that obtain the final part by removing material from the stock part. In this method, also called additive layer manufacturing, the product is created by adding layer by layer. AM developers do not intend to replace the traditional method of stock removal production. The main target is to be able to overcome jobs that are impossible to produce or involve serious difficulties with traditional methods. In this respect, AM has brought a great innovation to the advanced manufacturing industry because it can easily produce topologically optimized geometries and completely eliminates the need for fixture design and modeling, which has become an inevitable business in sectors such as aviation [20,21]. In Figure 3.5, the distribution of AM in 2020 according to its usage areas is given [22].

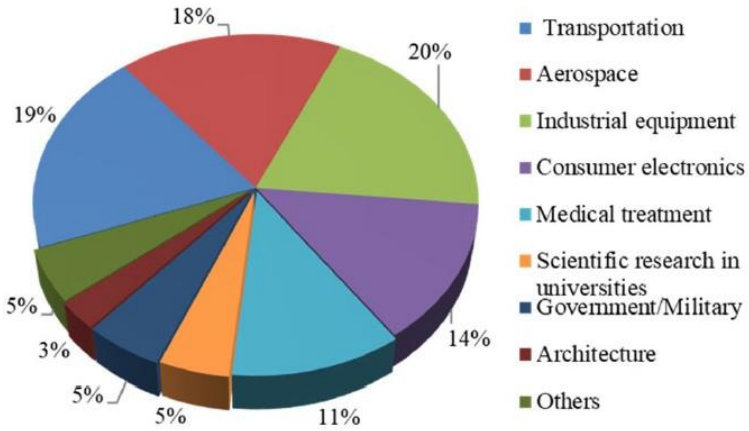

Figure 3.5. The distribution of AM usage areas.

3.2.2. The Types of Additive Manufacturing

Developers have come up with dozens of different types of AM in the last few decades. Although these types use quite different methods from each other in the background, it is the processes and materials that can be used to distinguish them in practice [23]. Figure 3.6 presents the 7 accepted main types of AM according to ASTM [24].

Powder Bed Fusion	•Selective thermal fusion of powder bed using a laser or an electron beam
Directed Energy Deposition	•Wire or powder is extruded from nozzle and completely melted by an electron beam or a laser
Binder Jetting	•Deposition of liquid bonding agent droplets to a powder bed
Sheet Lamination	•Sheets of material are bonded to form an object
Material Extrusion	•Material is extruded by a heated nozzle
Material Jetting	•Deposition of build material droplets by an inkjet print head
Vat Photopolymerization	•Selective curing of liquid photopolymer using light activated polymerization

Figure 3.6. Main additive manufacturing categories with description.

Many different manufacturers have developed additive manufacturing systems using various technologies and working methods, due to the fact that it is a new technology and has a high potential to improve production. For this reason, although AM is known as a way of manufacturing by simply adding material layer by layer, it contains many types and different methods within them [25]. If we are to categorize in general, the main types of AM; Binder Jetting, Direct Energy Deposition, Material Extrusion, Material Jetting, Sheet Lamination, Vat Polymerization and Powder Bed Fusion. Under these general categories, Stereolitography (SLA), Fused Deposition Modeling (FDM), Laser Melt Deposition (LMD), Electron Beam Melting (EBM), Selective Laser Sintering (SLS), Selective Laser Melting (SLM), Direct Metal Laser Sintering (DMLS) are known as the most common AM methods today [26]. In Figure 3.7, symbolic representations of some of the most commonly used methods are given [27]. These methods differ from each other by criterias such as the type of material used, the way of the material is deposited or solidified, layer thickness, and measurement precision.

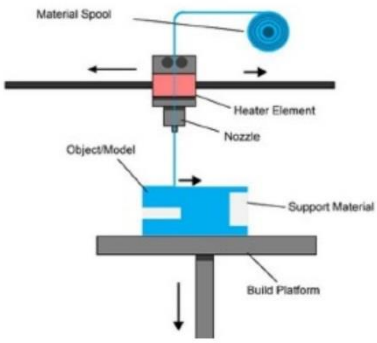

Fused Deposition Modelling

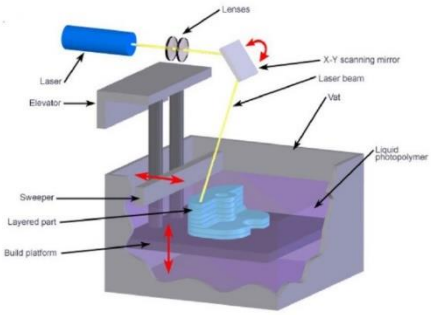

Stereolithography

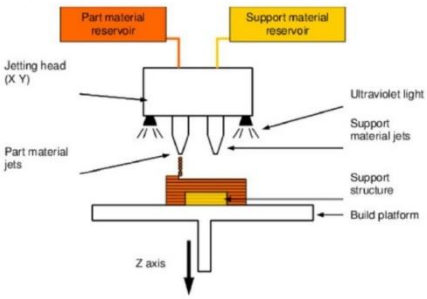

Inkjet Printing

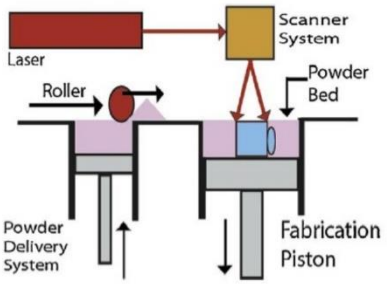

Laser Powder Bed Fusion

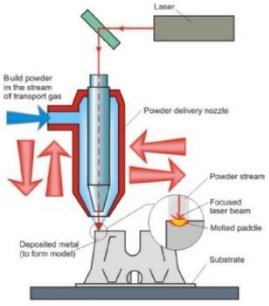

Laser Engineered Net Shaping

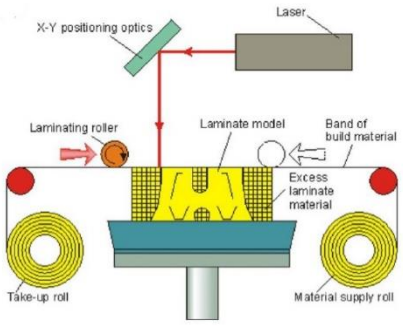

3DP (Binder Jetting)

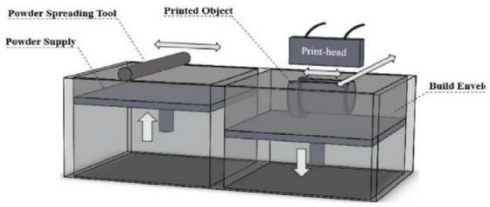

Laminated Object Manufacturing

Figure 3.7. Schematic represantations of common AM methods.

3.2.2.1. Powder Bed Fusion

Among the metal AM categories given in figure 3.8 [28], the Power Bed Fusion (PBF) method has become one of the most prominent methods in industrial use. This method simply involves the process of combining layer by layer by bringing the powders to the desired temperature by a power source. The sub-categories of laser used as a power source have found themselves under the title of L-PBF in the literature [29]. The methods in the L-PBF category chiefly vary according to the type of used material and working by sintering or melting. The most common methods are SLS, SLM and DMLS. While SLS is the most efficient method to produce polymer and ceramic materials, SLM and DMLS stand out when it comes to metal materials [30].

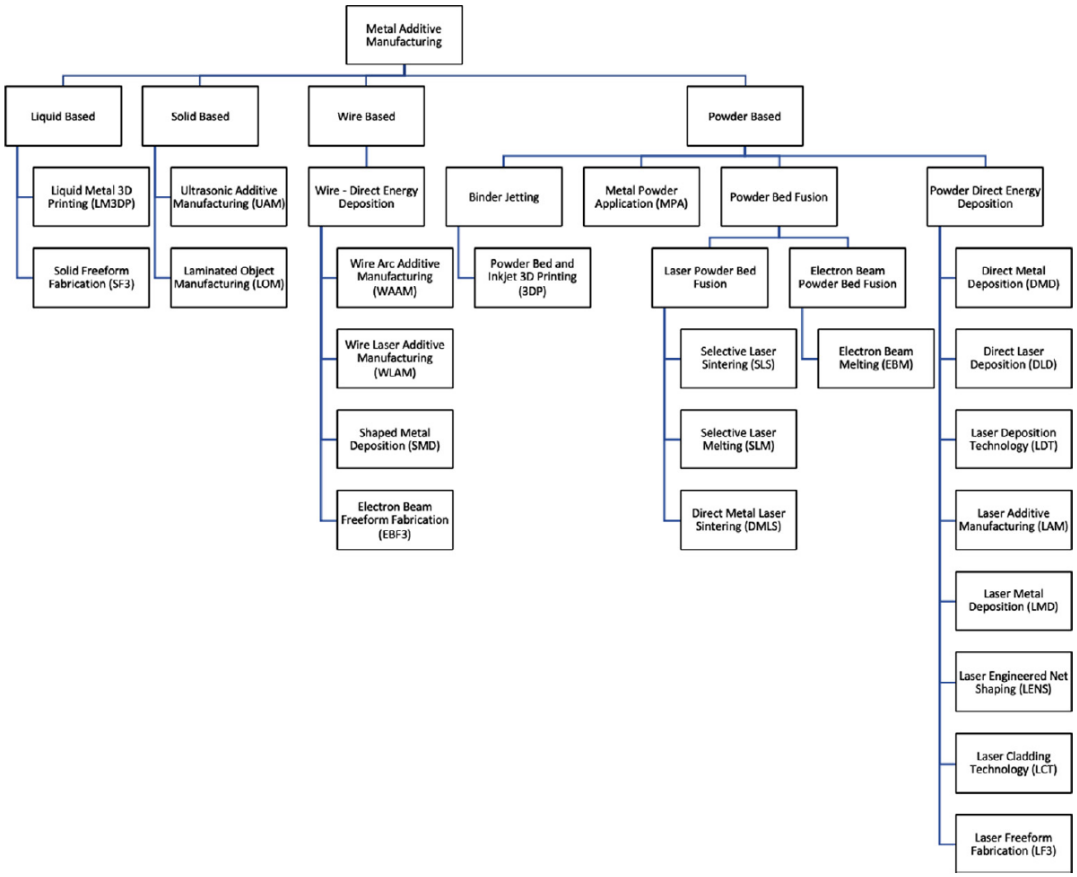

Figure 3.8. Classification of metal AM process.

The main difference of SLS method from SLM is combining powder particles by sintering rather than melting. This process has been tried on metal materials, but has not been successful as SLM. SLS method has come to the fore with the production of polymer, ceramic and some composite types. Because it can easily produce polymer bodies with complex geometries, it is still frequently preferred for rapid prototyping. However, it has become used for real production purposes in many important industries including aerospace [31].

Since there are various melting points in alloys and composites, combining these materials by melting is not an efficient use. With the DMLS method, materials having various melting points can be easily manufactured thanks to the advantage of sintering [32]. For this reason, the SLM method was identified with the production of pure metals with a fixed melting point in its early stages. However, due to the fact that the part is fused together by melting completely, SLM has the advantages of less porous structures and less need for post-production processes compared to DMLS. These advantages have led researchers to work on the production of frequently used materials such as carbon steel with this method. Today, SLM has become a frequently used method, especially in the production of carbon steels. Today, SLM has an important place in the production of high-tech engine blocks, automotive and aircraft components [33].

As given in figure 3.9 [34], the working principle of L-PBF includes the continuation process that feeding each layer of powder particles to the table according to the specified layer thickness of the body given in the 3D cad file with the re-coating blade, flattening the fed layer by a roller, creating a powder bed, selectively heating the powder bed to the sintering/melting temperature by the laser beam, and combining this process layer by layer until the final product is formed [35].

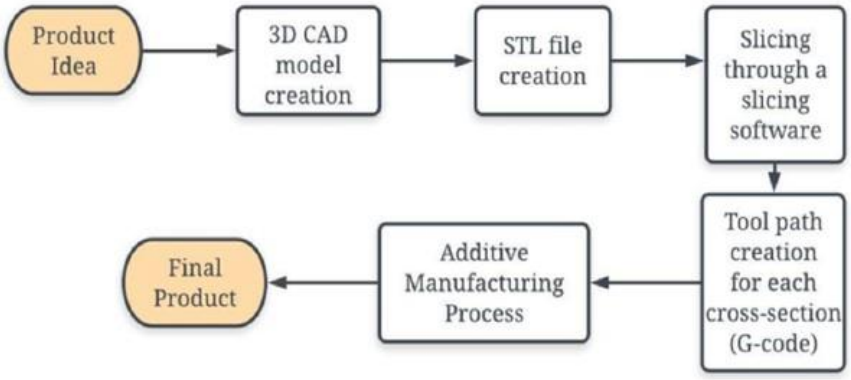

Figure 3.9. AM process workflow chart.

The biggest advantage of the L-PBF method is that metal and metal alloys can be produced in the desired geometry without any fixture design / production or any other prerequisites. In this way, it has an important place in the production of topologically optimized parts. It is widely used in areas where lightness and strength are important factors and research and development activities continue for these areas. In this respect, the sectors where it is mainly used are aerospace, automotive, military and medical sectors [36]. In Figure 3.10, the recent usage areas of AM and the forecast for the near future are given [37]. Considering the share of L-PBF, it can easily be said that it will continue to be the rising worth of value-added sectors in the coming years.

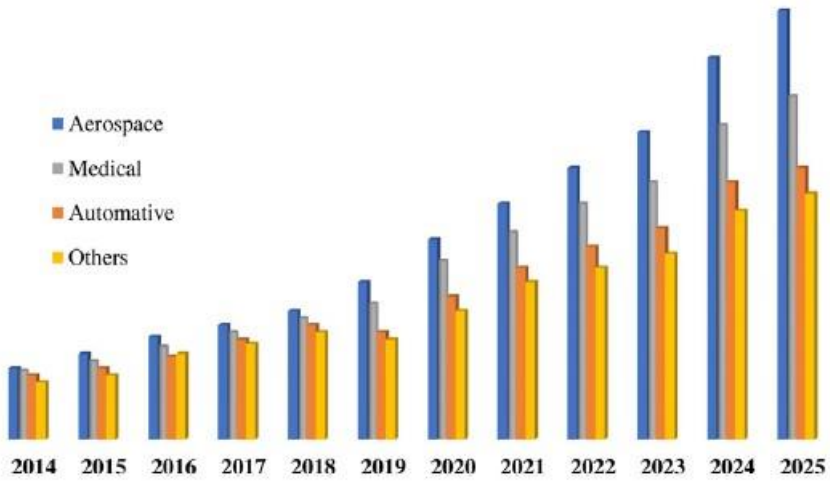

Figure 3.10. Forecast of market share by application area.

3.3. COMPUTER AIDED ENGINEERING

3.3.1. Finite Element Analysis

The finite element method can be defined as the numerical solution of partial differential equations. Its fundamental principle is to be expressed physical systems in terms of mathematical. Thanks to this method, the solution is simplified as much as possible, and even insoluble problems are made solvable. Since this method is based on simplification of the real system with assumptions and approximations, it does not promise accurate results [38]. But the finite element method, which has been used for structural strength analysis for more than 60 years, emerges as a method that can provide up to 98% accuracy with its technological development today. By means of this significant ratio, finite element analysis provides substantial convenience in solving engineering problems, minimizes prototype production and makes a great contribution to the speed of production. Linear and nonlinear static and dynamic problems can be solved with finite element analysis, which can be used in many package programs today [39].

3.3.1.1. Linear Static Analysis

Physical systems often contain nonlinear problems. Similarly, it is often not possible to be completely independent of time. However, since the basis of finite element analysis is to simplify the physical system as much as possible, by making certain assumptions, most systems can be considered linear and static. This is an important simplification that will save a lot of implementation steps, solver processor requirements and solution time [40]. One of the biggest factors in the transformation of a system into a non-linear problem is to undergo large deformation up to expose plastic strain. In such cases, solving the problem linearly leads to a more inaccurate results as the amount of deformation increases, as seen in Figure 3.11 [41]. In the light of this information, it can be said that a linearly solved problem can only make correct calculations up to the point where plastic deformation starts, that is, the yield strength. In addition, since all time-dependent variables will be disabled in the mathematical formula with the static assumption, it will be provided great benefit in

terms of calculation time and ease. In order to make this assumption, it is necessary to know the time the force is applied and the first natural frequency of the structure. If the frequency of the applied force is less than 1/3 of the first natural frequency of the structure, the system can be recognized static [42].

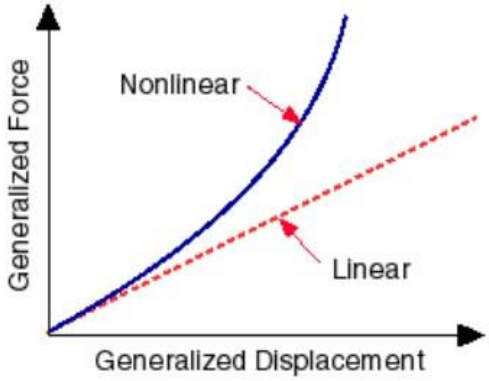

Figure 3.11. A comparison of linear vs nonlinear responses.

Before starting a finite element analysis, it is recommended to first perform a geometry simplification. At this stage, non-critical details and holes are filled. In this way, the finite element mesh can be formed ideally and thus more accurate data can be obtained as a result of the analysis. After the simplification process is complete, the material properties are defined. For linear static analyses, it is sufficient to define modulus of elasticity and Poisson's ratio. If the piece weight is to be used in the analysis, the density should also be defined. The next process is necessary for multi-body analyses. In these analyses, it is requisite to specify the contact relationships before creating the finite element mesh. Instead of defining these relationships one by one, giving general contact relationships also provides very successful results in current software. The selection of body elements such as shell and beam, which is very beneficial for the solution when used in the right place, should also be made without generating the mesh. Then, boundary conditions which will be mathematically included in the system are defined. The most important of these are the fixings that must be defined so that the structure does not undergo rigid body dynamics and the loading conditions included in the working principle of the system. With the completion of these processes, the finite element mesh, which can be called the most vital stage of the finite element analysis, can be generated [43].

A large number of various mesh elements such as hexahedron and tetrahedron for solid bodies, and quadrilateral and triangle for two-dimensional bodies such as shells and beams can be selected to obtain the best mesh. The finite element mesh can be generated according to either a first-order or a second-order polynomial. Since more nodes will be formed in the second-order mesh structure, it becomes possible to obtain more precise results. The adaptive mesh offered as an option allows gradually thinning the mesh, starting from a coarser size, instead of creating a small mesh size for the entire model. Thus, it becomes easier to reach the solution by decreasing the number of elements and nodes [44]. By performing these steps, the preprocessing is completed and the finite element analysis can be solved. Since the sparse matrix method, which can be used in simple operations of the finite element method, takes a very long time in large systems, finite element analysis package programs usually obtain numerical solutions using the Newton-Raphson method. Because of all the simplifications and the iterative solution method, 98% accuracy is promised instead of the exact correct result [45].

The equation used in the solution of linear static finite element analysis is expressed as Equation 3.1 in its most basic form. In this equation, F represents the force vector applied to the system, K represents the stiffness matrix containing material and geometric properties such as Young's modulus, moment of inertia, cross-sectional area, and u represents the displacement vector. In linear static structural analyses, the unknown is the displacement and this value is obtained as a result of the analysis. In consequence, other desired values such as stress and strain are produced by mathematical formulas. The finite element solver calculates the values for each node of the mesh and interpolates the values at the common nodal points of each element to reveal the element values. As mentioned above, the finite element number of the regions where critical values occur can be increased in order to measure more precisely. One way to understand if we have obtained the proper mesh is to solve the analysis with a relatively coarse mesh element size and then gradually refine it to observe the convergence of the results. When it is noticed that it does not converge further, the mesh can be considered sufficient. Apart from this method, quality parameters that can be observed to measure mesh quality are also available in finite element software [46].

$$\{F\} = [K] \cdot \{u\} \tag{3.1}$$

Reaction forces can be observed to confirm the analysis results. Whether the reaction forces formed in the fixing regions meet the forces applied to the system or not, provides important clues about the correct construction of the analysis and giving correct results. The important point to be considered in the interpretation of linear static analysis results is that the analysis can only provide accurate results in the elastic region. Because the analysis was carried out assuming that the structure will not be deformed enough to be exposed to plastic deformation, which is called large deformation. For this reason, the results of the analysis should be interpreted in the region up to the yield point and it should be known that permanent deformations such as rupture and fracture cannot be observed here. One of the most meaningful results that can be read is how safe the system is according to its yield strength. In ductile materials, the factor of safety is obtained by dividing the yield strength by the highest stress occurring in the structure [47]. Figure 3.12 shows the elastic region and plastic region separated by the yield point in ductile materials such as steel [48].

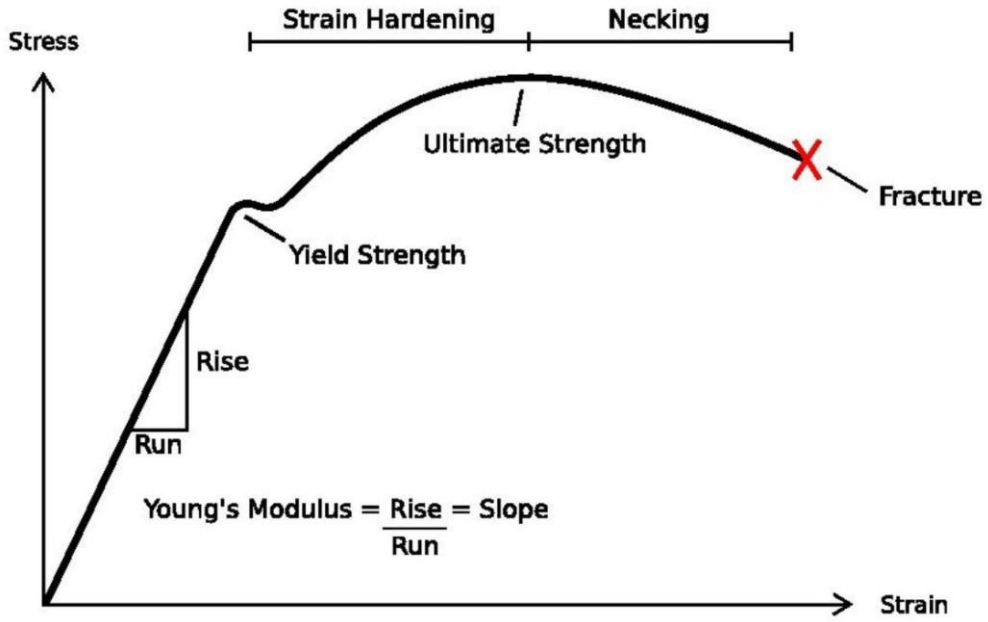

Figure 3.12. Stress-Strain curve of a ductile material.

3.3.2. Topology Optimization

Structural optimization, which includes size, shape and topology optimizations, has an adventure of approximately 100 years. Since topology optimization can be produced completely independent of the initial design, it gives the most efficient results in terms of mass and strength compared to the other two methods [49]. However, as it is very difficult to manufacture the geometries obtained by this method with traditional methods, it has not been able to show the expected effect in the design and production areas until recently. In the last 20 years, in parallel with the developments in the field of additive manufacturing, many studies have been carried out in the field of topology optimization and it has shown a rapid development [50]. In the topology optimization study for traditional manufacturing, the geometry is redesigned according to the design criteria for manufacturing after the first optimization result is obtained. This geometry is re-optimized as it may deviate from the optimized values. Generally, very productive results cannot be obtained at the end of this iterative process [1]. The design criteria for additive manufacturing allow production with the most optimum results as it minimizes design constraints. With this aspect, additive manufacturing has opened a new era in the field of topology optimization [51].

One of the most important steps in the topology optimization study is to determine the goals and constraints correctly. Although each type of topology optimization reaches a solution with a different formula, this step is common for all methods. Because topology optimization is not a parametric process, if the constraints are not determined, an impractical and useless geometry is obtained. Thus, it is especially important to determine the regions that need to remain stable in order to apply fixation or loads. In addition, some values such as volume, natural frequencies, displacements and reaction forces can also be set as constraints to remain constant or within a certain range. In order for the optimization study to achieve its purpose, goals such as reducing the volume, increasing the stiffness, reducing the displacement, increasing the first natural frequency or reducing the reaction force can be determined for desired rates [52].

3.3.2.1. Density Based Method and SIMP

Topology optimization is trying to find the most efficient form of a geometry's placement in a given volume, depending on certain constraints, by means of a mathematical formula. There are types of topology optimization based on various optimization formulas created with different parameters. The main ones are homogenization method, level set method, phase field method, evolutionary structural optimization and density based method [53]. Studies in this area are still continuing intensively and new developments are occurring in most of these methods. Two of the most prominent among these methods are Bi-directional Evolutionary Structural Optimization (BESO) derived from evolutionary structural optimization and Solid Isotropic Material with Penalization (SIMP) derived from density-based method [54].

The SIMP method has emerged as the most suitable method for finite element-based use and has been integrated into many commercial finite element software. In the SIMP method, density values are assigned to each element in the finite element model, representing 0 empty element and 1 solid element, and the optimization process is performed iteratively with a function dependent on the elasticity modulus [55]. Due to its popularity and usefulness, a lot of academic studies have been done about the SIMP method and it has been developed especially with finite element analysis software to make it more efficient. In the current usage, the density value should be different from 0 in order for the mathematical function to be processed stably and for the finite element analysis to be solved correctly for optimization. The element density value is expressed by ρ. The smallest empty element represents the expression ρ_{min}. The reason why this value should be different from 0 can be easily understood from the calculation of the stiffness matrix according to the SIMP method given in Equation 3.2. If 0 is given for the empty element, it will be difficult to get meaningful results from such equations used in the formulation. The modulus of elasticity also varies, as the material density varies between elements. The modulus of elasticity for each element is calculated as in Equation 3.3. As it can be understood from this equation, the penalty factor p forces each element to be an empty or solid element, reducing the effect of elements with intermediate densities.

There are also different equations that are used according to the set goals and constraints. The SIMP method algorithm tries to reach the given goal by an iterative process. These iterations continue until the changes in the goal functions meet the desired convergence criteria [56].

$$K = \sum_{e=1}^{N} \left[\rho_{min} + (1 - \rho_{min})\rho_e^p\right] K_e \tag{3.2}$$

$$E = E_0 \cdot \rho^p \tag{3.3}$$

The SIMP method is used in leading finite element analysis softwares such as Ansys, Simulia Abaqus, Altair Hyperworks, SW Simulation. Since it has been determined from previous studies that the value of 3 gives the best result for the penalty factor p, this value is usually defined by default, and different values can be used optionally [57]. The interpolation scheme for different values of the penalty factor p is given in Figure 3.13 [58]. This diagram shows the case of E/E0 relative to ρ^p using Equation 3.3. Element sizes should be as small as possible in order to obtain efficient results in the SIMP method. The recommended values are approximately one quarter of the ideal values used in a linear static analysis. In addition, it is highly recommended that the aspect ratio not exceed 1.1 in order to ensure the sensitivity between the elements [59].

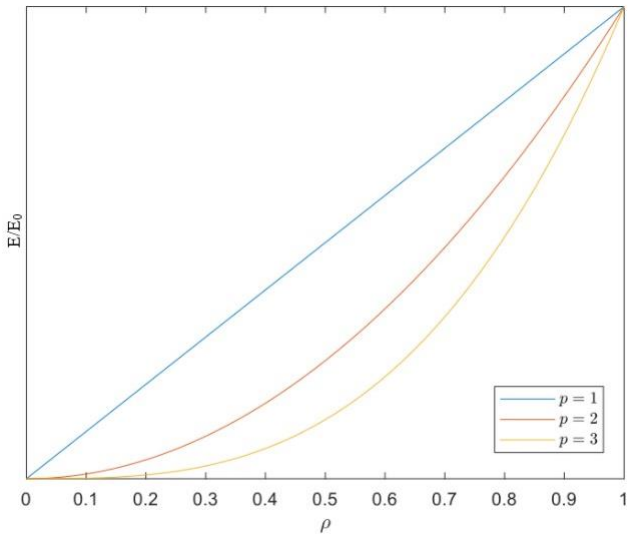

Figure 3.13. Simp interpolation scheme.

PART 4

METHODOLOGY

In this study, which deals with the design of automotive components for additive manufacturing, case studies are carried out on the lower control arm of the front suspension system used in pickup type vehicles.

4.1. MODEL DEFINITION

In the case studies, the suspension system preferred in vehicles such as toyota hilux, mercedes x-class and nissan navara is based. The reason for choosing the suspension system used in pickup type vehicles is that these vehicles have a high load carrying capacity. Thus, applications were carried out with both curb and gross weights and significant differences could be observed. By taking advantage of the catalog information of these vehicles, the curb and gross weights were accepted as 2 tons and 3 tons, respectively []. The lower control arm in the suspension system of this type of vehicle was modeled in SOLIDWORKS and shown in Figure 4.1.

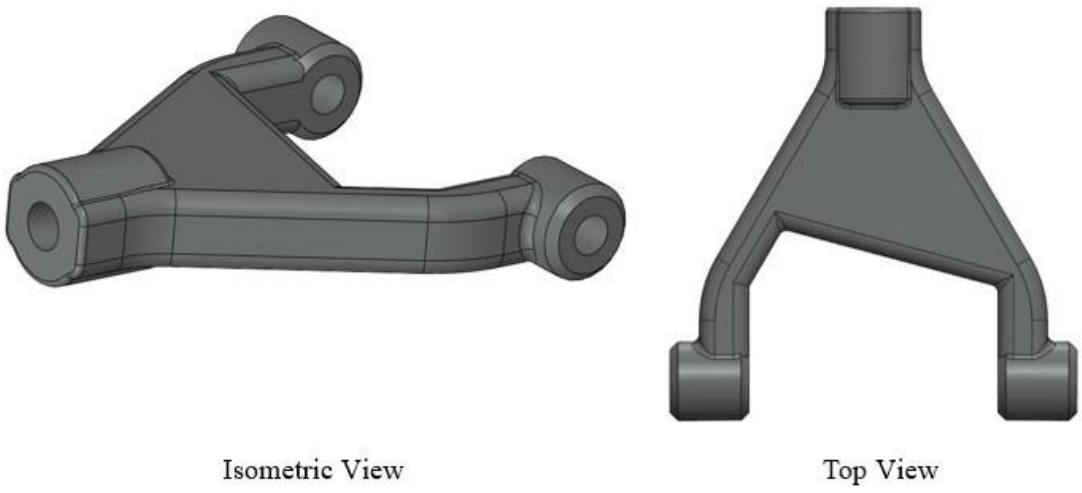

Figure 4.1. 3D model views.

4.2. APPLICATION DETAILS

Within the scope of this thesis, a number of computer aided engineering applications were carried out in a certain order. The work started with the selection of the material to be applied and the definition of the mechanical properties of the material to the model. Boundary conditions were defined by making relevant assumptions, and the forces acting on the model in the case of curb and gross weights of the vehicle were calculated for the loading conditions. After the finite element mesh was generated, linear static and modal analyses were performed. Then, topology optimization applications were performed with different goal strategies and limitations. An optimized model was obtained by interpreting and reverse engineering the graphical models that emerged as a result of these applications. The applications were concluded with the linear static and modal analysis of this model.

4.2.1. FEA Definitions

In the study, linear static analysis was used to calculate stress and displacement, and modal analysis was used to calculate natural frequencies. FEA studies were performed in the SOLIDWORKS Simulation environment.

4.2.1.1. Approximations and Assumptions

Since the topology optimization studies would be applied on a single body, necessary simplifications were fulfilled before FEA. Powertrain and dampers such as coil spring were passivated. Fixture was applied as 6 dof from the center of rotation assuming the spring was rigid to restrict rigid body motion. The force was applied as half of the weight acting on the front wheels from the wheel coupling.

4.2.1.2. Material Properties

Various materials can be preferred in vehicle suspension systems [60]. In this study, the commonly used mild steel material was based [61]. The mechanical properties of the mild steel material were given in Table 4.1.

Table 4.1. Material properties of Mild Steel.

Young's Modulus (E)	$2{,}1 \times 10^5$ MPa
Poisson's Ratio(v)	0,28
Yield Strength (σ^{YS})	220,594 MPa
Tensile Strength ($^{\sigma TS}$)	399,826 MPa
Density (ρ)	7800 kg/m^3

4.2.1.3. Boundary Conditions

In Figure 4.2, fixtures and loadings were given by green and purple arrows respectively. By applying the simplifications mentioned in section 4.2.1.1, fixtures were made from the rotation axes. The force acting on a front wheel at the curb and gross weight of the vehicle was applied vertically from the wheel joint.

Using Equations 4.1 and 4.2, the force on one front wheel of the vehicle was calculated [62]. In these calculations, the curb and gross weights of the vehicles given in section 4.1 were accepted as 2 tons and 3 tons, respectively. In this type of vehicles, the load acting on the front axle was accepted as 35% in the curb weight state, and 30% in the gross state since the luggage load added.

$$F = \mathrm{m} \cdot \mathrm{g} \tag{4.1}$$

$$F_{a\ front\ wheel} = \mathrm{F} \cdot \mathrm{FWR} \cdot 1/2 \tag{4.2}$$

Forces acting on single front wheel in case of curb and gross weight were calculated in Equations 4.3 and 4.4.

$$F_{curb} = 2000 \cdot 9{,}81 \cdot 0{,}35 \cdot \frac{1}{2} \approx 3500N \tag{4.3}$$

$$F_{gross} = 3000 \cdot 9{,}81 \cdot 0{,}30 \cdot \frac{1}{2} \approx 4500N \tag{4.4}$$

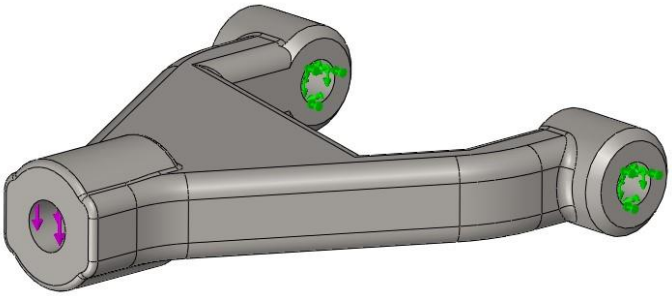

Figure 4.2. View of applied fixture and load.

4.2.1.4. Generating Mesh

Second order mesh was preferred because the regions where critical stresses occur were important in the analysis. Although a sufficiently fine mesh was generated for finite element analyses, a finer mesh was applied for topology optimization as mentioned in section 3.3.2.1. The parameters used were presented in Table 4.2.

Table 4.2. Mesh details of FEA and topology optimization studies.

Linear Static and Modal Analysis		**Topology Optimization**	
Mesh element type	Solid Mesh	Mesh element type	Solid Mesh
Mesher	BCB Mesher	Mesher	BCB Mesher
Mesh quality	Second order	Mesh quality	Second order
Min element size	1 mm	Min element size	1 mm
Max element size	5 mm	Max element size	3 mm
Element ratio	1,4	Element ratio	1,1
Total element number	99074	Total element number	373374
Total node number	144895	Total node number	529412

The meshed models obtained for FEA and topology optimization were given in Figure 4.3.

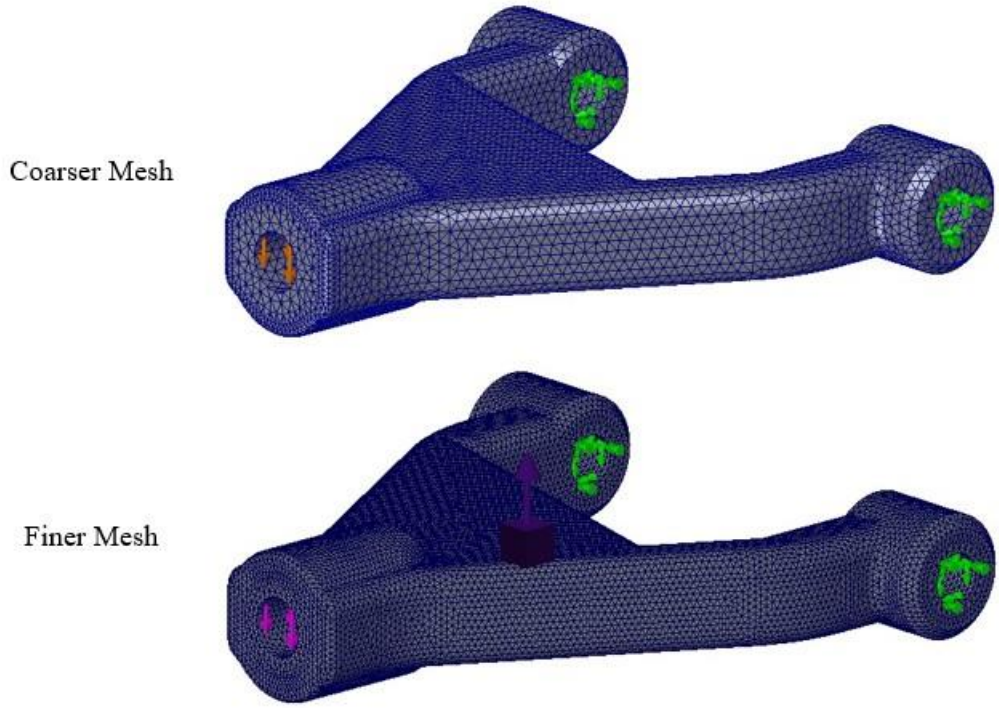

Figure 4.3. Meshed models for FEA and topology optimization.

4.2.1.5. Solving Process

The software used in the analysis provides users with the FFE plus iterative solver and 3 direct solver options including direct sparse, large problem direct sparse and intel direct sparse. For large models with a great number of dofs, it is recommended to use the iterative solver, which uses considerably less ram than direct solvers. Since all analyzes were performed on a single body in this study, it is appropriate to prefer a direct solver. The workstation, where the analyzes were carried out, has an Intel® i7-10870H processor and 32 GB ram. For this reason, intel direct sparse solver, which provides the most efficient multi-core usage and solution time of this system, was chosen in all analyses [63].

4.2.2. Topology Optimization Definitions

Topology optimization studies were performed in the topology study module of SOLIDWORKS Simulation, which solves using simp formulation. In this module, in addition to the definitions made for linear static analysis, goals, constrains and manufacturing controls were determined. Topology study strategies applied in this thesis have been shown in Table 4.3.

Table 4.3. Topology optimization strategies.

Strategy A	**Optimization Goal**	**Minimize Mass**
	Constraints	Displacement is less than 0,3 mm
		Frequency mode 1 is less than 500 Hz
	Manufacturing Controls	Half symmetry by top plane
Strategy B	**Optimization Goal**	**Minimize Maximum Displacemet**
	Constraints	Reduce mass by %15
		Frequency mode 1 is less than 500 Hz
	Manufacturing Controls	Half symmetry by top plane
Strategy C	**Optimization Goal**	**Best Stiffness to Weight Ratio**
	Constraints	Reduce mass by %15
		Frequency mode 1 is less than 500 Hz
	Manufacturing Controls	Half symmetry by top plane

4.2.2.1. Goals and Constraints

In the topology study, the software offers the user 3 different goal options. These options were implemented with various goal and constraint preferences to obtain the model that would provide the most efficient values in both loading conditions. The result obtained by defining both loads from the load case manager menu was considered as validation. Briefly, both strategies A and B were applied for the two different loading conditions. In addition, strategy C was applied under the multiple load cases. Thus, 5 different models were acquired.

4.2.2.2. Manufacturing Controls

The application provides the user with manufacturing controls such as adding a preserved region, determining the minimum and maximum thickness control, determining the de-mold direction and determining the symmetry plane. In all topology studies applied in this study, we defined the top plane as the symmetry plane. Thus, we obtained symmetrical geometries with respect to the top plane.

4.2.2.4. Solving Process

The solver options mentioned in section 4.2.1.5 are also available for topology optimization. In the topology study, intel direct sparse solver was used, which gives the most efficient results in terms of CPU and ram usage as long as the memory is sufficient. The software's solver menu also allows the user to select the regions to be preserved and the number of iterations to be applied. For this study, the number of iterations was chosen as automatic, which continues the solution until the desired goals are achieved. Preserved regions were selected the regions with loads and fixtures.

PART 5
RESULTS

The models obtained from the performed analyses were given in Table 5.1 by naming them according to different loading conditions and optimization states.

Table 5.1. Classification of the models acquired as a result of the analysis.

		Curb Weight	Gross Weight	Multiple Load Case
Without Optimized	Linear Static	**MS1**	**MS2**	
	Natural Frequency	**MF1**		
With Optimized	Minimize Mass	**MM1**	**MM2**	
	Minimize Maximum Displacement	**MD1**	**MD2**	
	Best Stiffness to Weight Ratio			**MC1**

5.1. FEA RESULTS

Before the topology study, finite element analyses were implemented to the existing model. The stress, displacement and natural frequency values obtained as a result of these analyses were used as goals and constraints in topology studies.

5.1.1. Linear Static Analysis Results

Stress and displacement values are the most frequently used parameters in topology optimization studies. For this reason, linear static analyses were made at the beginning of the study and these values were found. Two separate analyses were performed for curb and gross weight. In these studies, the model fixed from the chassis joint was loaded from the wheel joint. Loads were applied in the direction of gravity, taking into account the weight of the vehicle.

The critical stress regions that emerged in the analysis made for the MS1 model representing the curb weight are shown in Figure 5.1. As a result, 70.51 MPa von mises stress was measured.

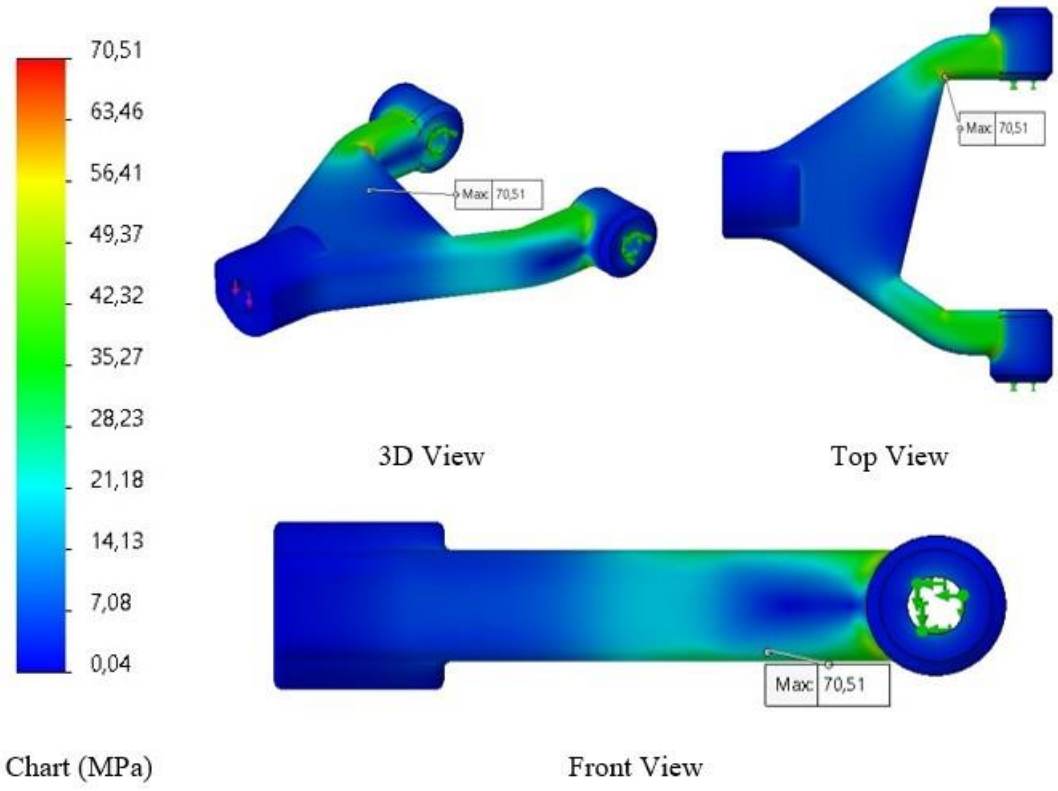

Figure 5.1. MS1 von mises stress result.

During topology optimization studies, displacement values often provide more useful parameters than stress values. The reason for this is that the stress values are higher than the actual value in models that do not have smooth curvature surfaces. However, correct results can be found by obtaining the surface curvatures properly by reverse engineering process. Consequently, the initial stress values are used only for comparison with the final model. In topology studies, the displacement value is used as a parameter.

The displacement plots that emerged in the analysis made for the MS1 model representing the curb weight are shown in Figure 5.2. In the analysis result, it was seen that the amount of displacement increases linearly from the chassis joint to the wheel joint. The maximum displacement of 0,22 mm was measured at the wheel joint, which is the loading area, while a 0 displacement value was measured in the chassis joint, which is the fixation area.

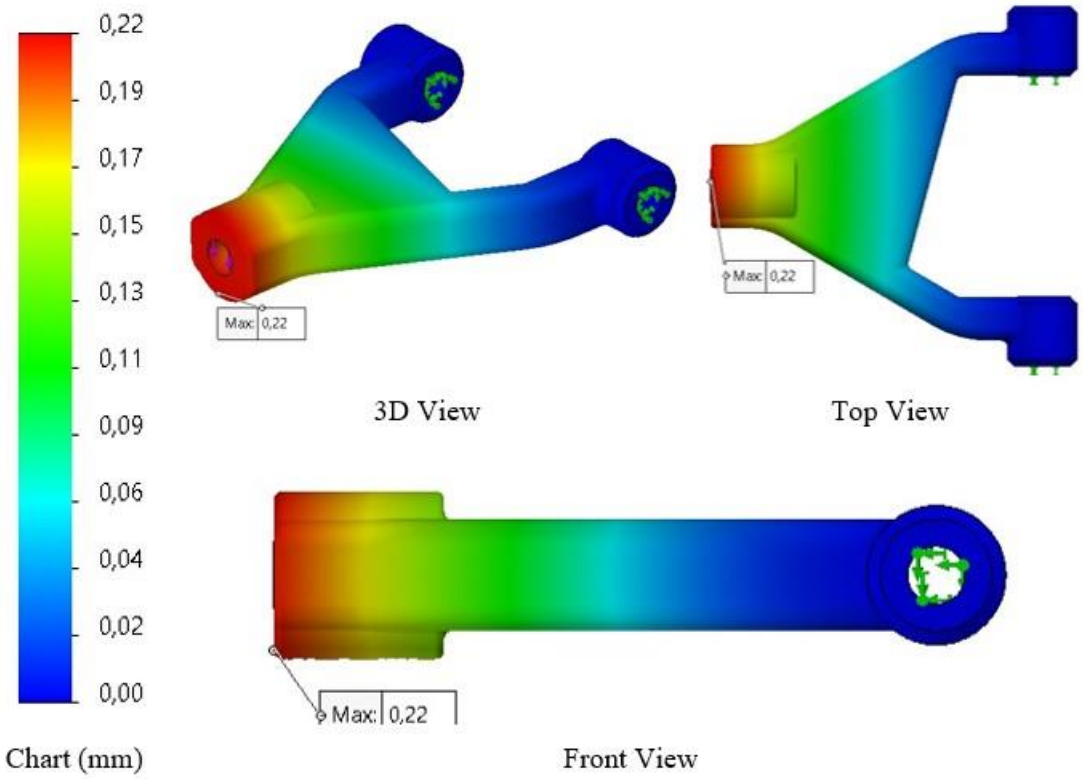

Figure 5.2. MS1 displacement result.

The critical stress regions that emerged in the analysis made for the MS2 model representing the gross weight are shown in Figure 5.3. As a result, 90,65 MPa von mises stress was measured.

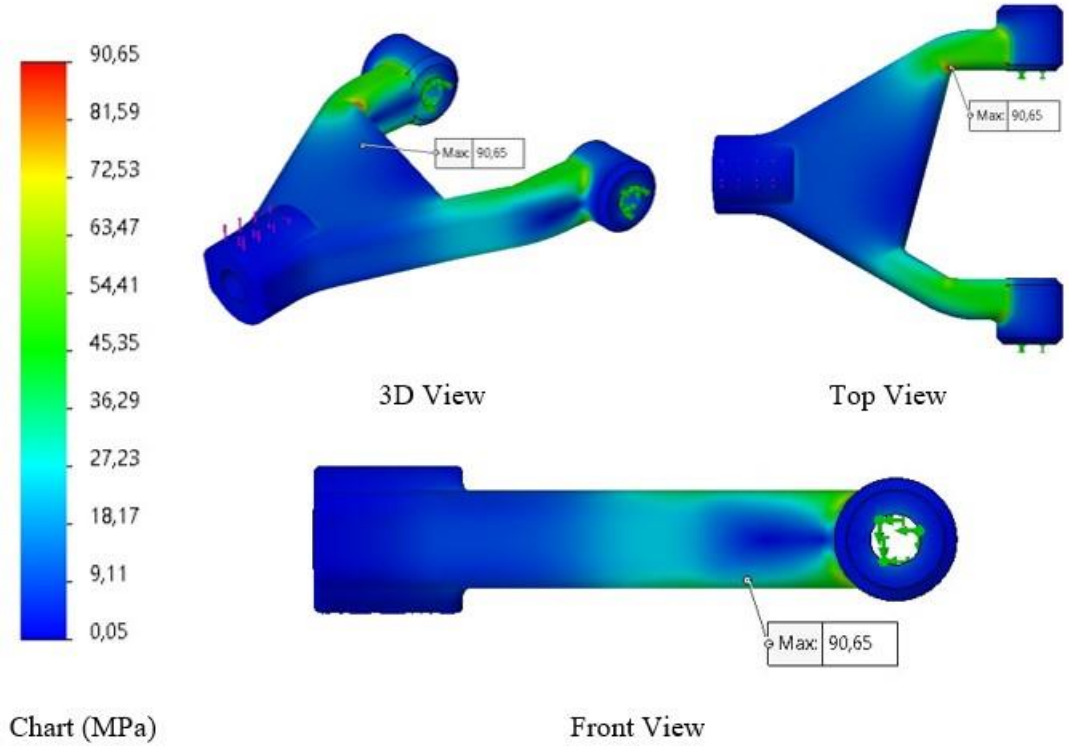

Figure 5.3. MS2 von mises stress result.

The displacement plots that emerged in the analysis made for the MS2 model representing the gross weight are shown in Figure 5.4. In the analysis result, it was seen that the amount of displacement increases linearly from the chassis joint to the wheel joint. The maximum displacement of 0,28 mm was measured at the wheel joint, which is the loading area, while a 0 displacement value was measured in the chassis joint, which is the fixation area.

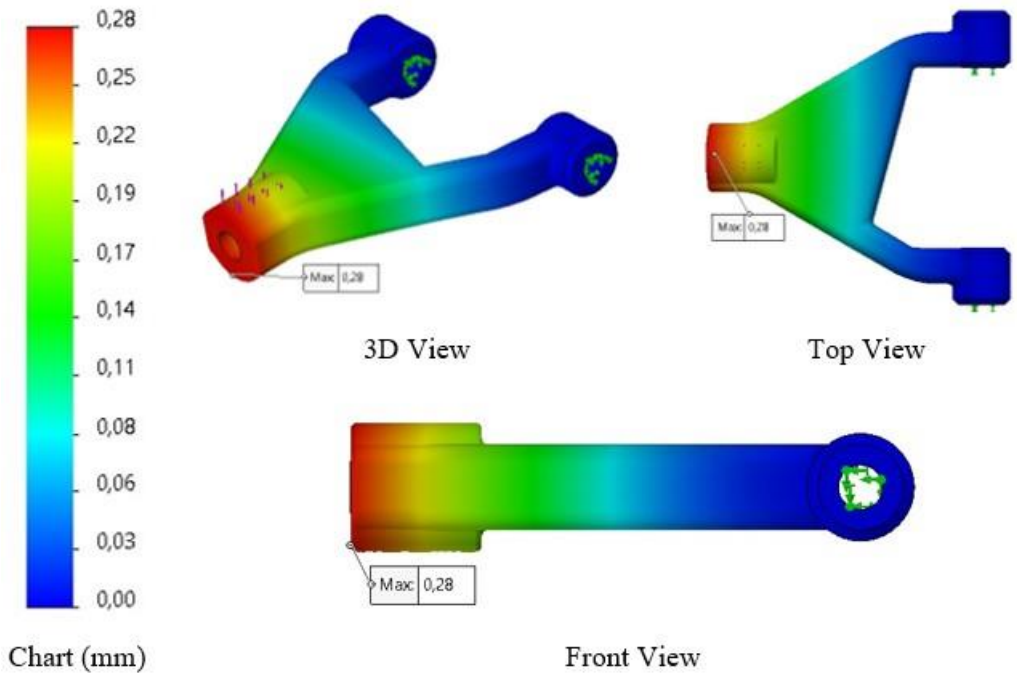

Figure 5.4. MS2 displacement result.

5.1.2. Modal Analysis Results

It is important to consider natural frequencies in the design phase of automotive components that are exposed to long-term operation. For this reason, modal analysis was carried out both to use it as a parameter in topology studies and to compare it with the final model. It was considered sufficient to measure the first five natural frequencies in the modal analysis implemented without force.

When the results were examined, it was observed that the natural frequency formed in the direction of application of the force was the first mode. The first natural frequency value to be used in topology studies was found to be 407.64 Hz. The values for the first five modes are presented in Table 5.2.

Table 5.2. Frequency and period list of MF1.

Mode No.	Frequency(Rad/sec)	Frequency(Hertz)	Period(Seconds)
1	2.561,3	407,64	0,0024531
2	9.952,3	1.584	0,00063133
3	12.928	2.057,6	0,000486
4	14.199	2.259,8	0,00044251
5	18.466	2.939	0,00034026

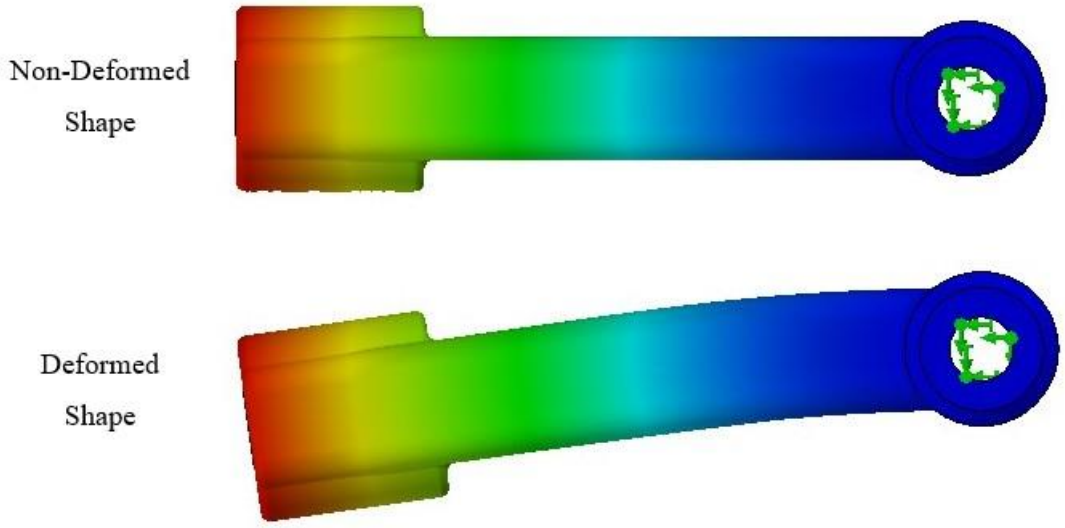

Figure 5.5. Deformation shape of MF1.

5.2. TOPOLOGY STUDY RESULTS

Topology optimization studies were implemented under three different strategies: Strategy A, B and C. With Strategy A and B, 4 different results were obtained for 2 different load cases. Strategy C, on the other hand, was handled as a single study covering both load cases with the load case manager. Thus, five topology studies appeared.

The models that emerged as a result of the topology studies applied under three different strategies and the weight, stress, displacement and natural frequency values of these models were given under this title.

The simp method used in applications works according to the method of keeping the necessary mesh elements and excluding the mesh elements that are not needed. Therefore, the models that appear during studies do not have smooth shapes. In case this would cause the data to be high, the parameters used in the optimization criteria were taken a little high.

5.2.1. Weight Results of Strategy A

Strategy A was implemented with the goal of minimize mass. As stated above, as the optimization criterion, displacement value was preferred instead of stress. In linear static analyses before the topology study, 0.22 and 0.28 mm displacement were measured for the curb and gross weight, respectively. A maximum displacement constraint of 0.30 mm was set for this strategy. In addition, in order to be able to control the natural frequency and observe the natural frequency in the resulting model, the constraint for frequency mode 1 to be less than 500 was also defined. Finally, the solving process was carried out with the manufacturing control of half symmetry by top plane.

In the curb weight study of Strategy A, a material mass of 5,29 kg was achieved with a %51 decreasing rate. Topology variable stress value resulted in 151,87 MPa and topology variable displacement value resulted in 0,30 mm. Frequency mode 1 value was found to be 480,85 Hz. The plots showing the values on the model were given in Figure 5.6.

In the gross weight study of Strategy A, a material mass of 7,31 kg was achieved with a %33 decreasing rate. Topology variable stress value resulted in 163,22 MPa and topology variable displacement value resulted in 0,30 mm. Frequency mode 1 value was found to be 481,58 Hz. The plots showing the values on the model were given in Figure 5.7.

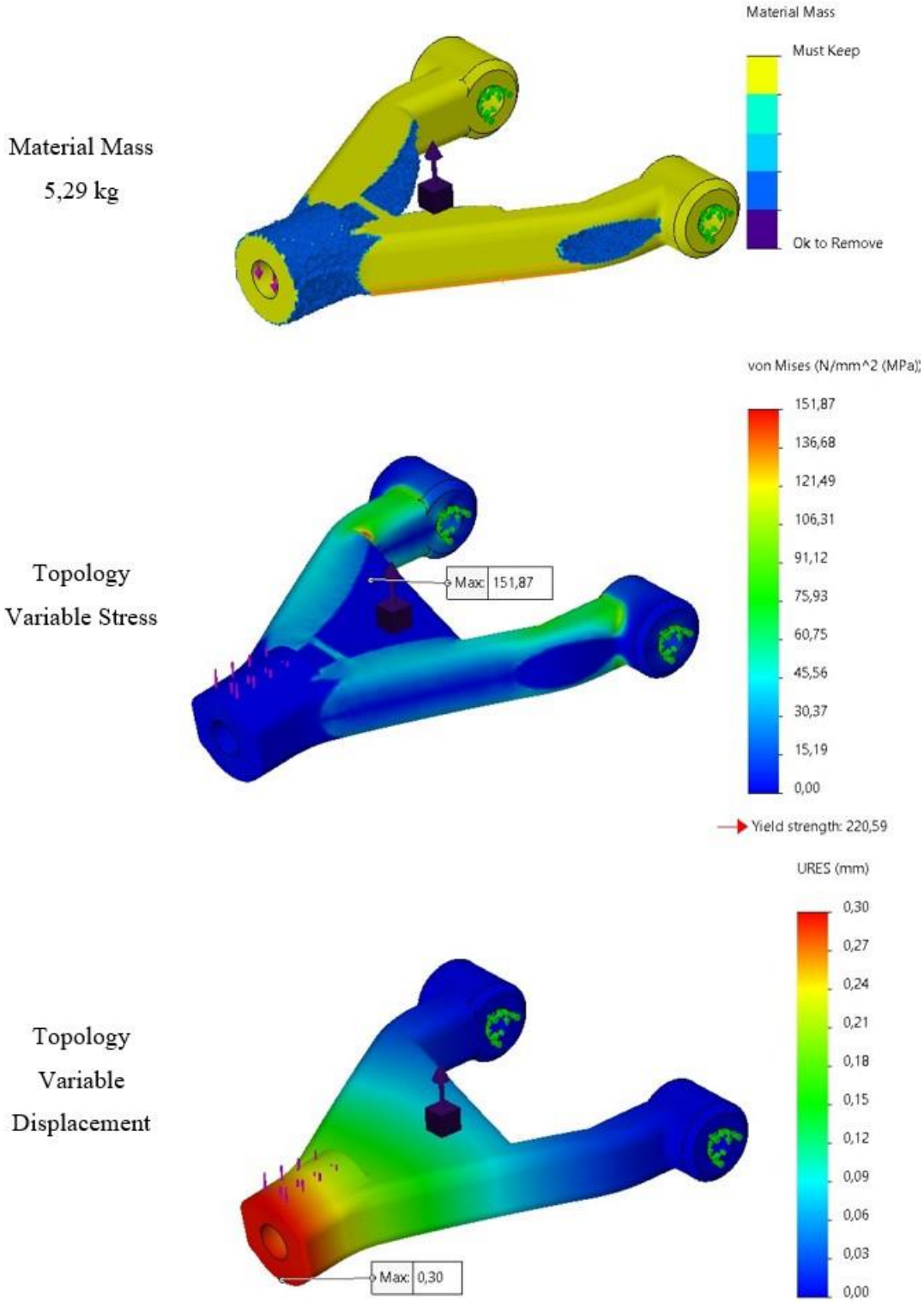

Figure 5.6. Results of MM1.

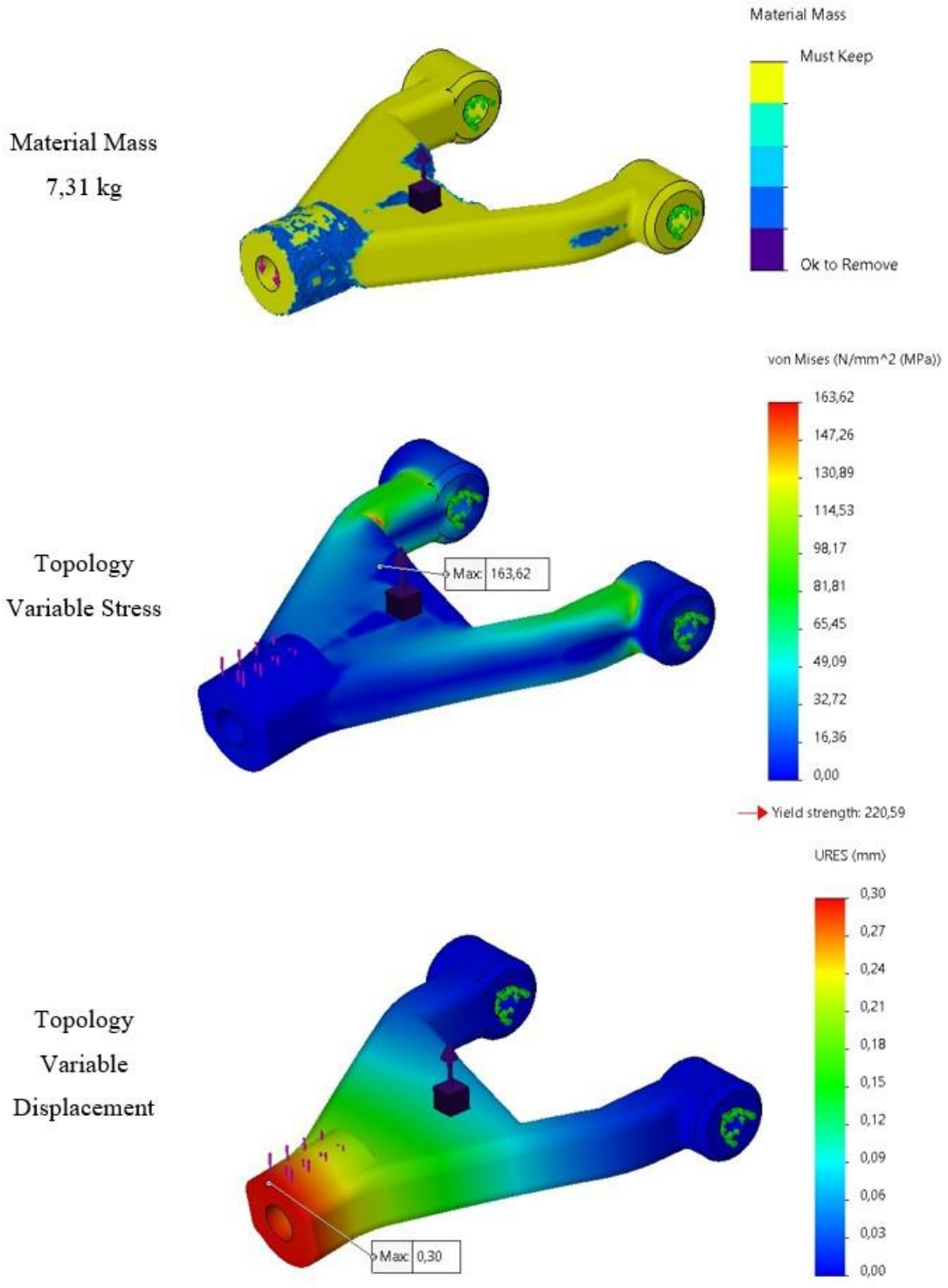

Figure 5.7. Results of MM2.

5.2.2. Weight Results of Strategy B

Strategy B was implemented with the goal of minimize maximum displacement. In the topology studies towards this goal, the least desired mass reduction constraint should be specified. Considering the values obtained in Strategy A, this value has been determined as 15%. In addition, in order to be able to control the natural frequency and observe the natural frequency in the resulting model, the constrain for frequency mode 1 to be less than 500 was also defined. Finally, the solving process was carried out with the manufacturing control of half symmetry by top plane.

In the curb weight study of Strategy B, a material mass of 8,19 kg was achieved with a %25 decreasing rate. Topology variable stress value resulted in 123,01 MPa and topology variable displacement value resulted in 0,22 mm. Frequency mode 1 value was found to be 463,6 Hz. The plots showing the values on the model were given in Figure 5.8.

In the gross weight study of Strategy B, a material mass of 9,31 kg was achieved with a %14 decreasing rate. Topology variable stress value resulted in 159,51 MPa and topology variable displacement value resulted in 0,28 mm. Frequency mode 1 value was found to be 446,71 Hz. The plots showing the values on the model were given in Figure 5.9.

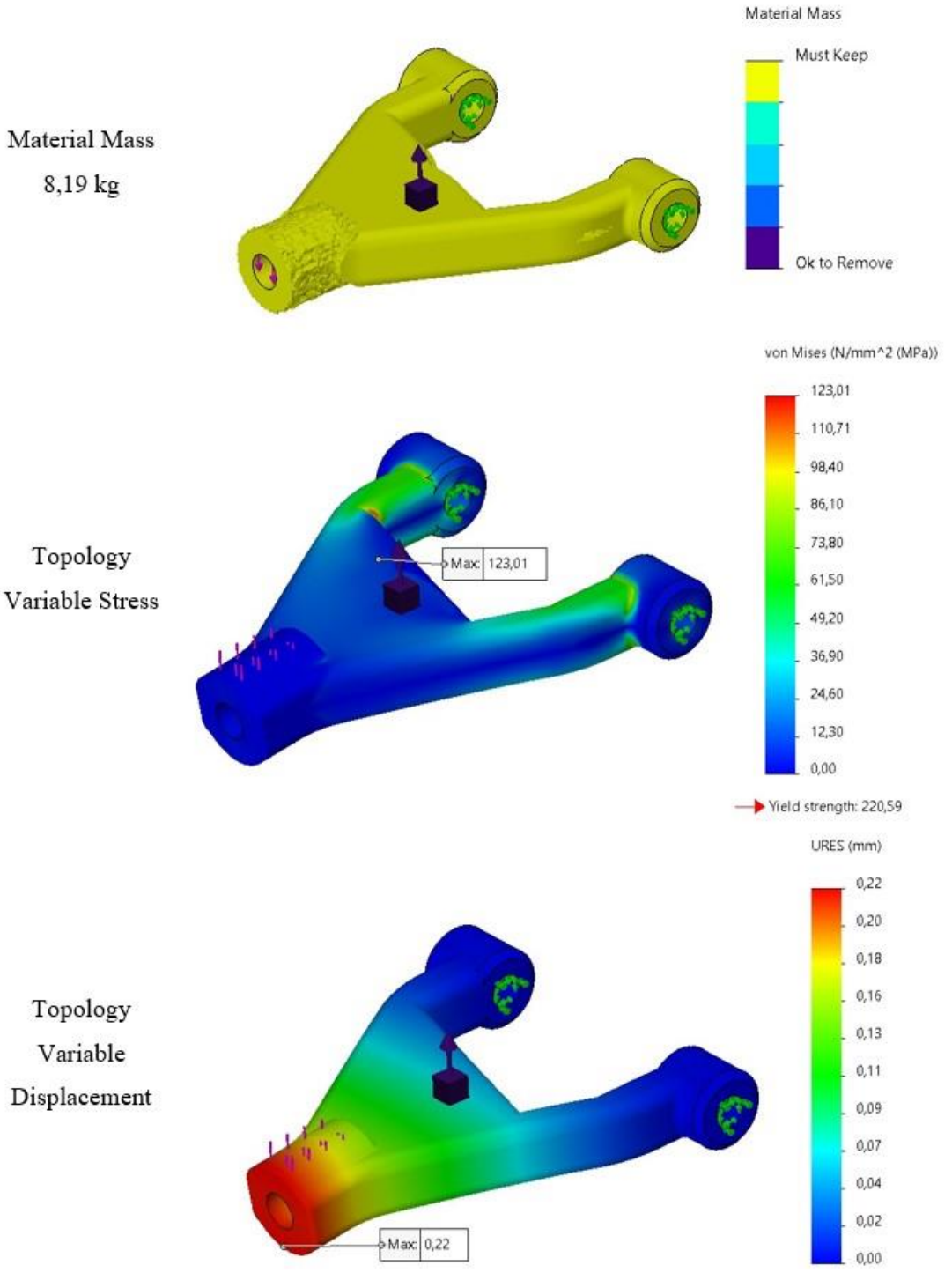

Figure 5.8. Results of MD1.

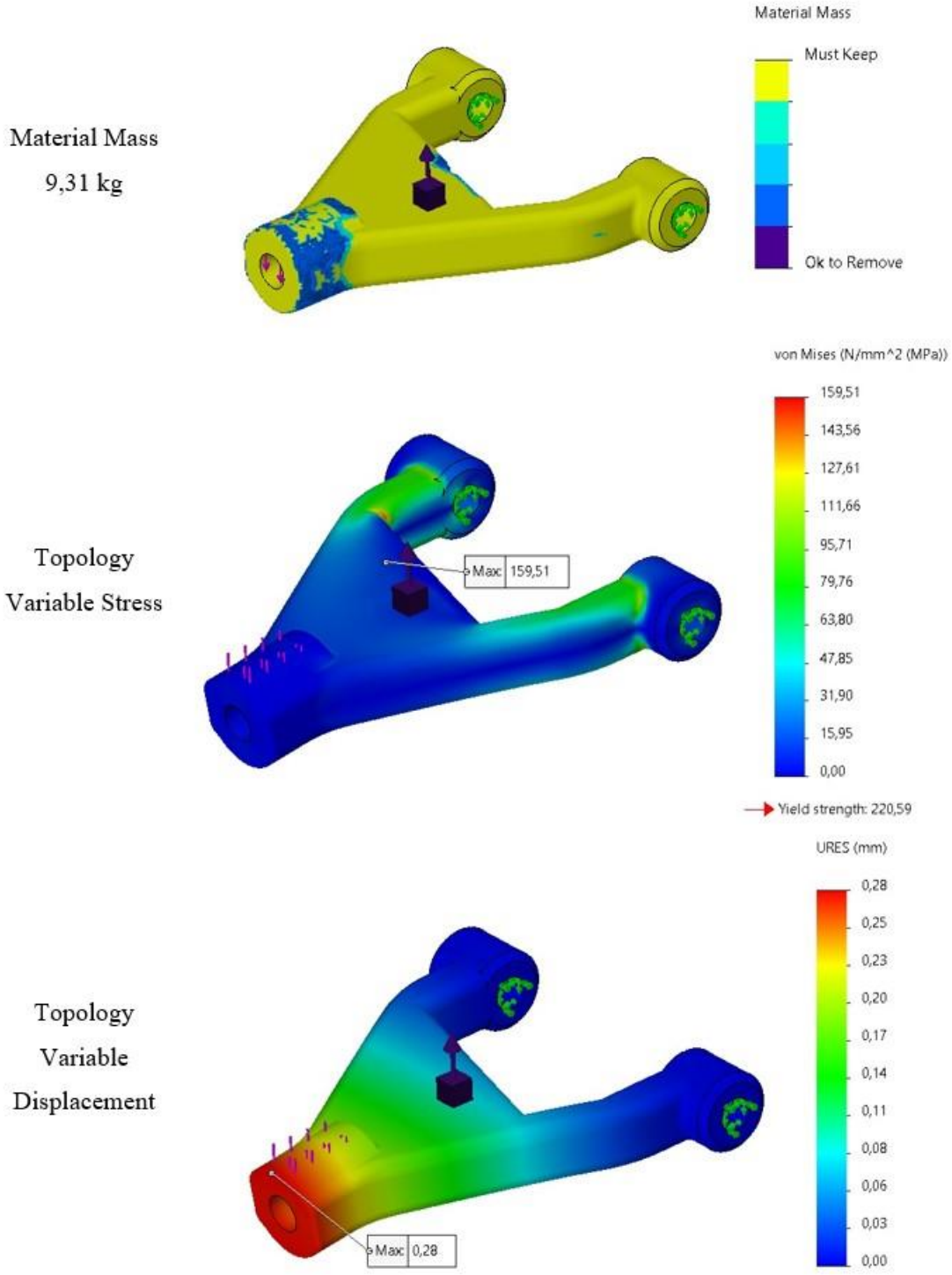

Figure 5.9. Results of MD2.

5.2.3. Weight Results of Strategy C

Strategy C was implemented with the goal of best stiffness to weight ratio. In the topology studies towards this goal, the least desired mass reduction constraint must be specified. This value was determined as 15% in terms of the result being compatible with strategy B. In addition, in order to be able to control the natural frequency and observe the natural frequency in the resulting model, the constrain for frequency mode 1 to be less than 500 was also defined. Finally, the solving process was carried out with the manufacturing control of half symmetry by top plane.

In the multiple load cases study of Strategy C, a material mass of 9,30 kg was achieved with a %14 decreasing rate. Topology variable stress value resulted in 124,76 MPa for curb weight and 160,41 MPa for gross weight. Topology variable displacement value resulted in 0,22 mm for curb weight and 0,28 mm for gross weight. Frequency mode 1 value was found to be 448.2 Hz. The plots showing material mass values on the model were given in Figure 5.10. The topology variable stress plots were given in Figure 5.11 and the topology variable displacement plots were given in Figure 5.12.

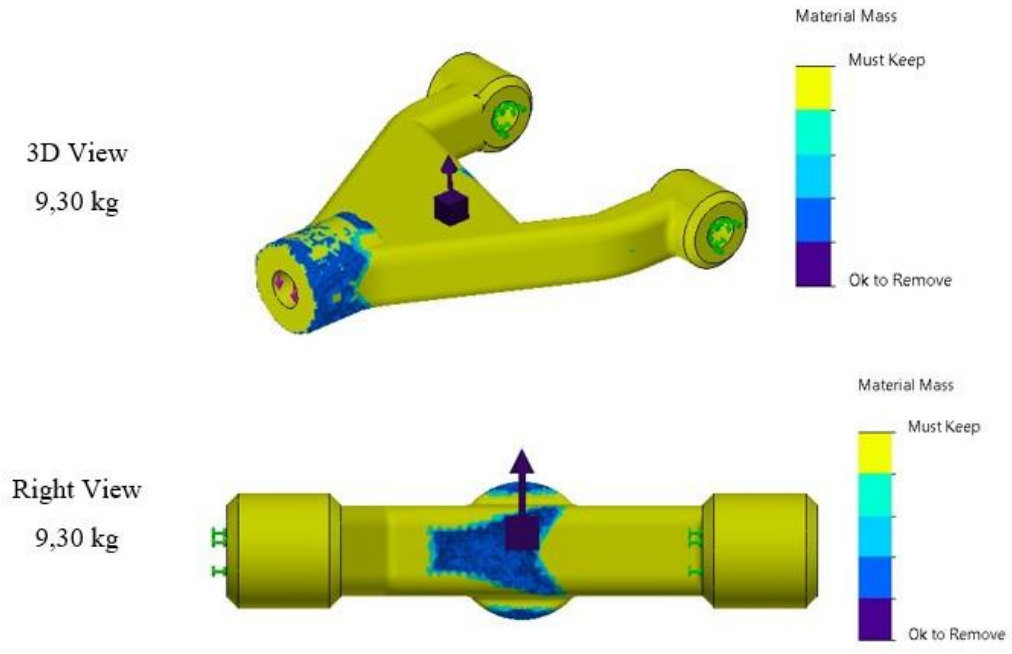

Figure 5.10. Material mass plots of MC1.

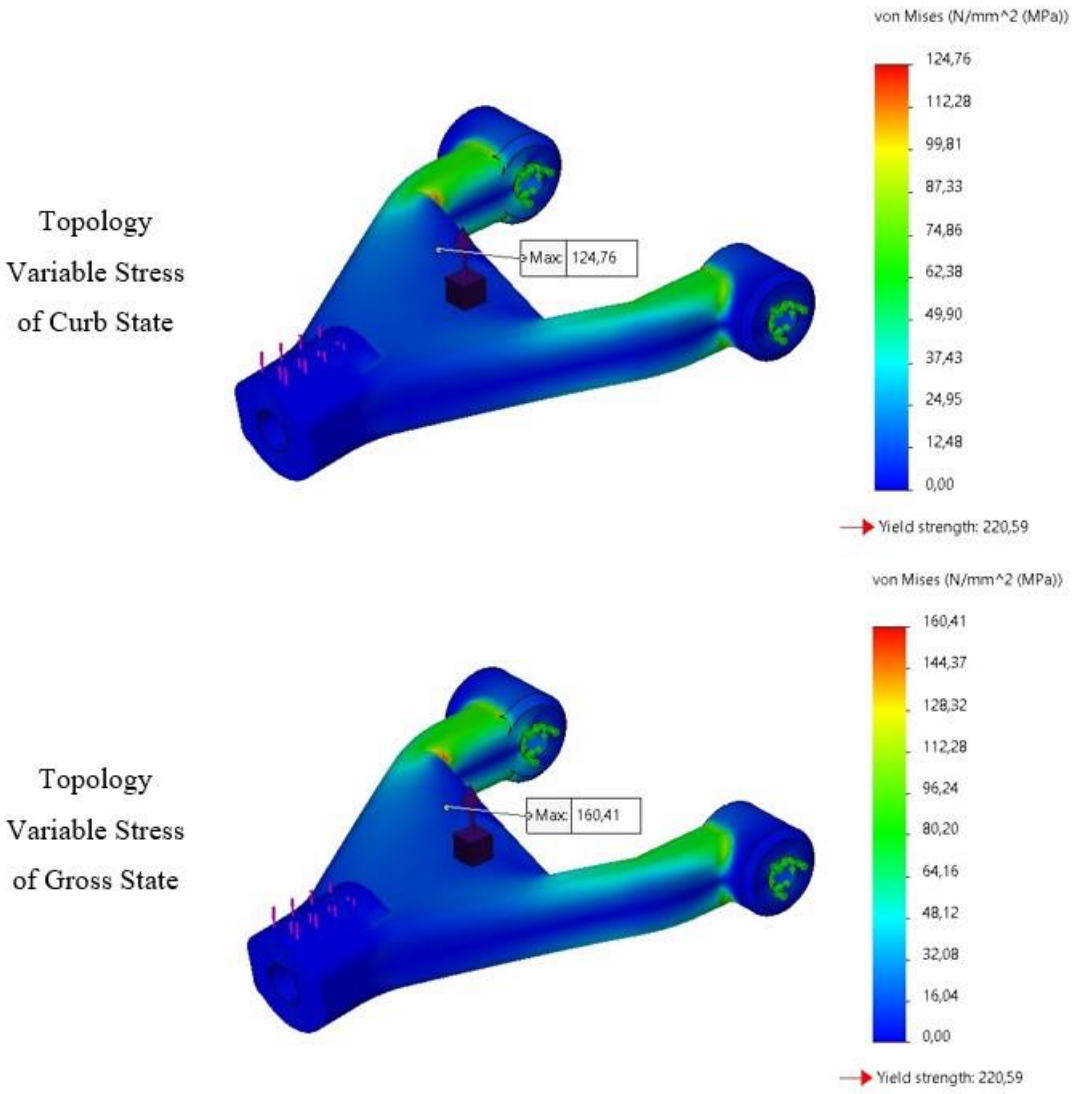

Figure 5.11. Von mises result plots of MC1.

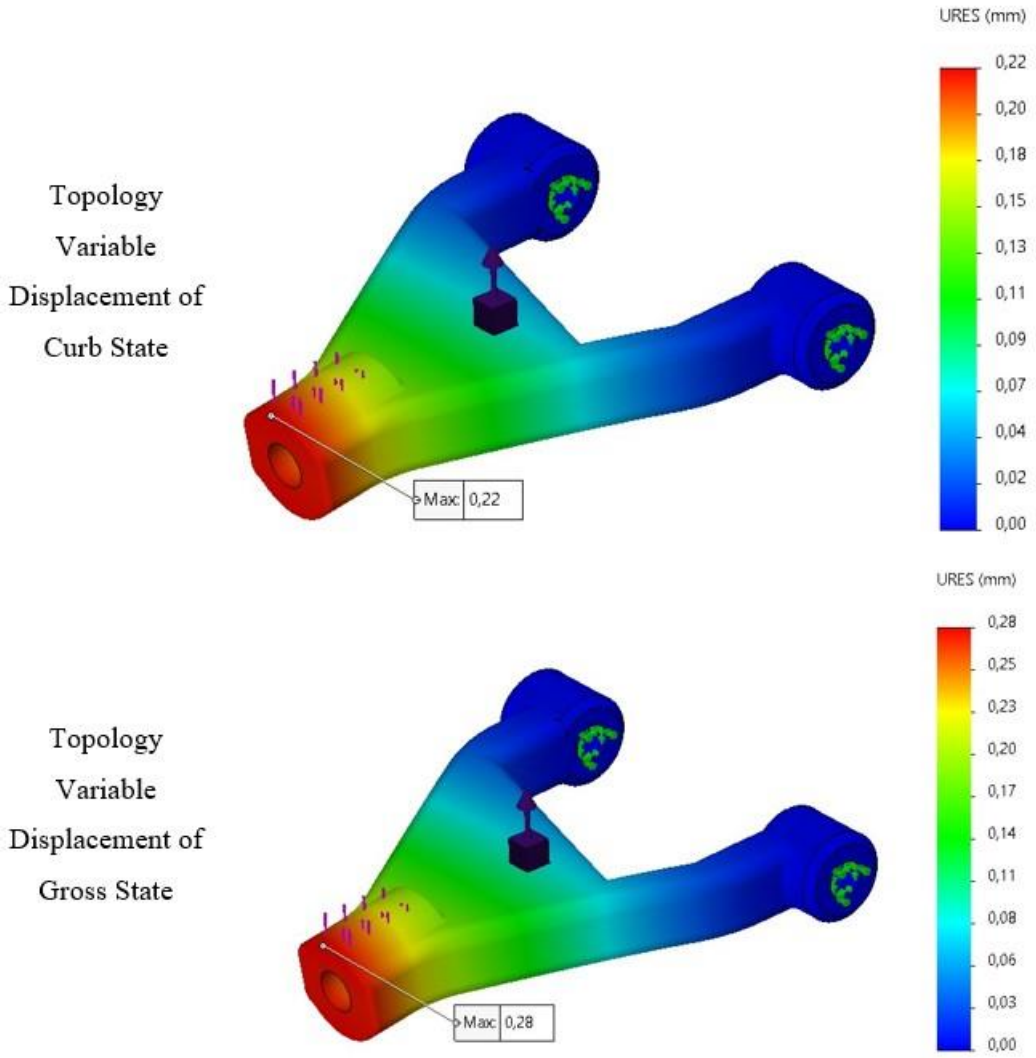

Figure 5.12. Displacement plots of MC1.

5.3. OPTIMIZED MODEL RESULTS

An optimized model was obtained by applying reverse engineering to the graphic bodies that emerged after the topology study. This model was validated by performing linear static and modal analyses.

3D View of Optimized Model

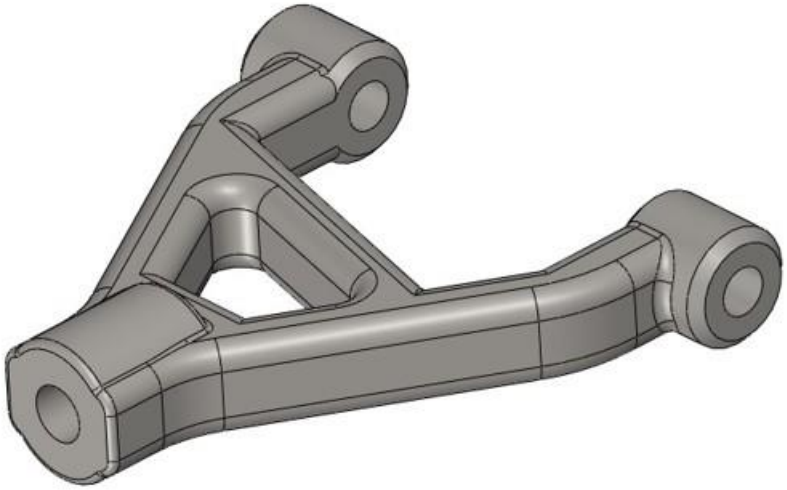

Top View of Optimized Model

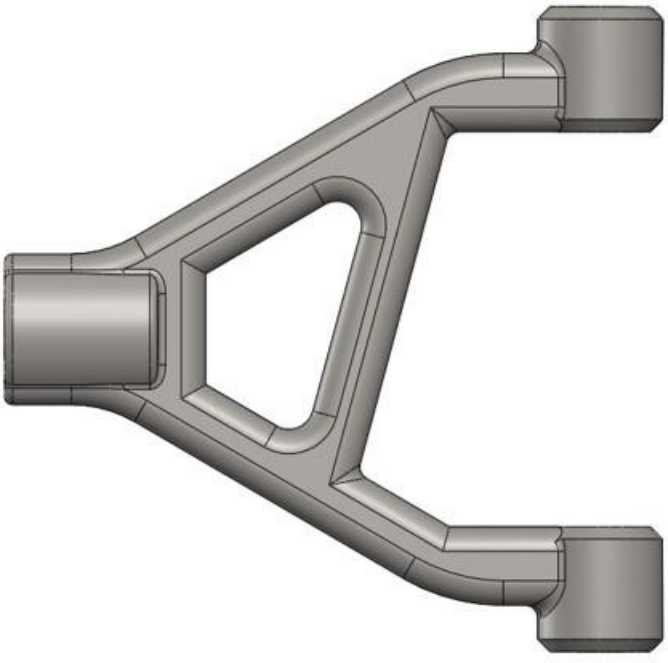

Figure 5.13. The views of optimized model.

5.3.1. Linear Static Analysis Results

The linear static analyses applied to the first model were made in the same way on the optimized model acquired by performing reverse engineering and conceptual design steps.

The critical stress and displacement regions that emerged in the analysis made for the optimized model representing the curb weight are shown in Figure 5.14. As a result, 69,01 MPa von mises stress and 0,24 mm displacement was measured.

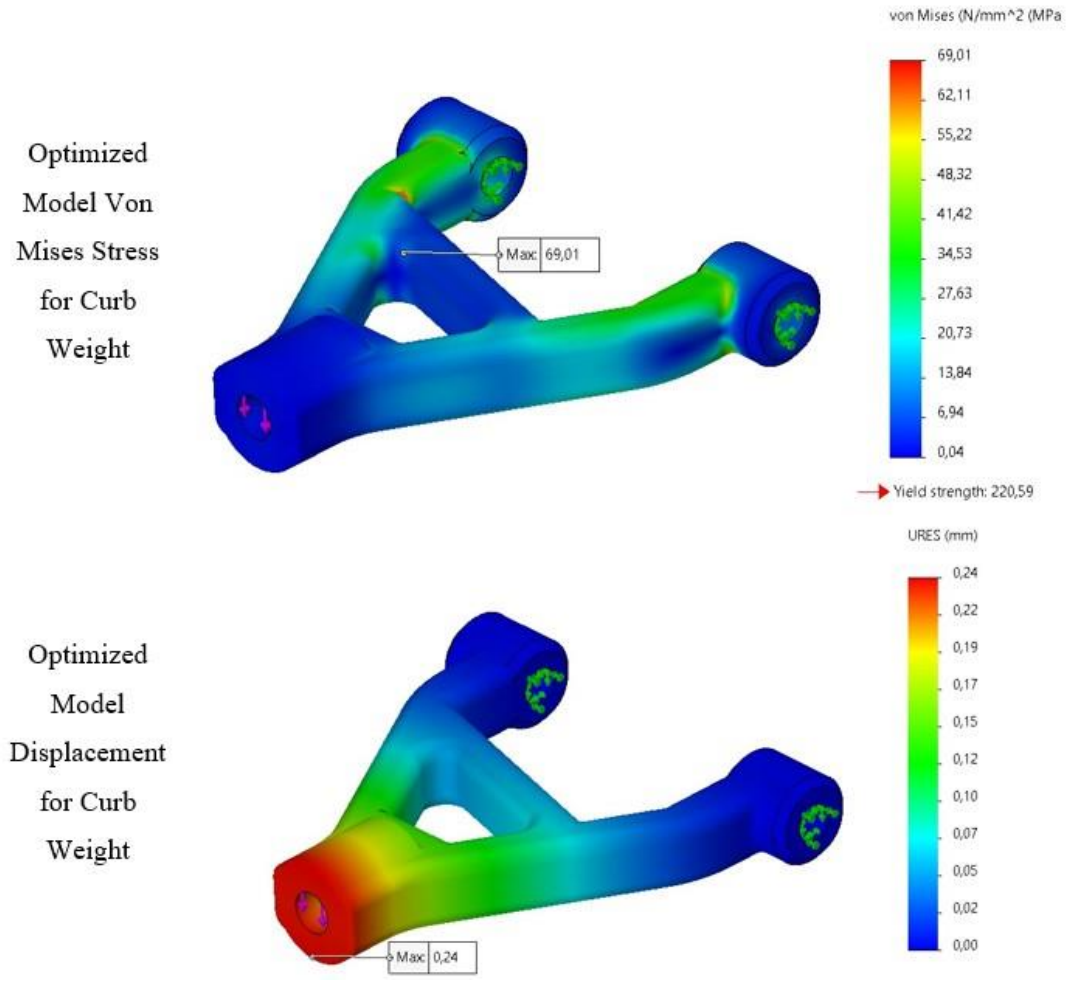

Figure 5.14. Curb weight result of optimized model.

The critical stress and displacement regions that emerged in the analysis made for the optimized model representing the gross weight are shown in Figure 5.15. As a result, 88,73 MPa von mises stress and 0,31 mm displacement was measured.

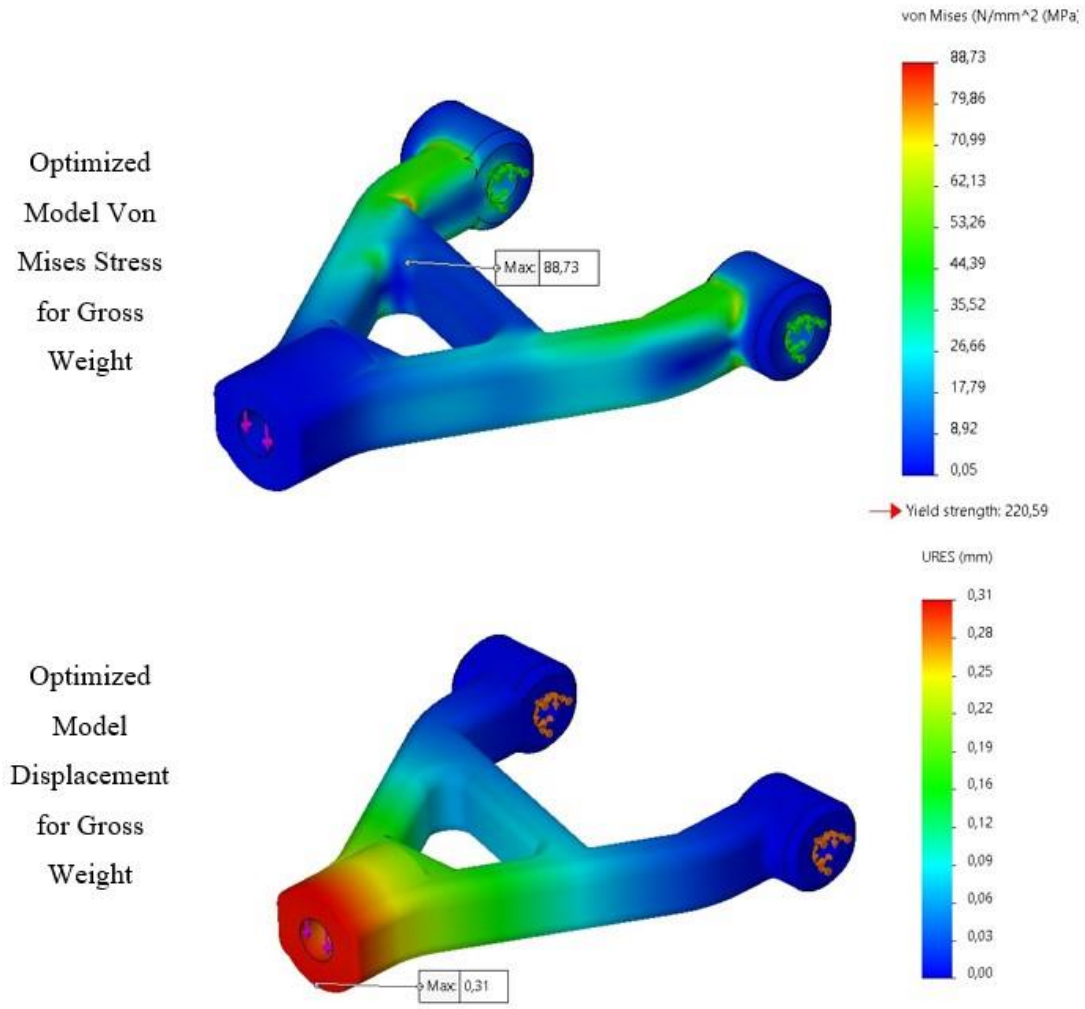

Figure 5.15. Gross weight result of optimized model.

5.3.2. Modal Analysis Results

The values for the first five modes are presented in Table 5.3. When the results were examined, the frequency mode 1 which was used all studies was found to be 423.28 Hz.

Table 5.3. Frequency of period list of optimized model.

Mode No.	Frequency(Rad/sec)	Frequency(Hertz)	Period(Seconds)
1	2.659,5	423,28	0,0023625
2	9.876,7	1.571,9	0,00063616
3	12.455	1.982,2	0,00050449
4	13.050	2.077	0,00048146
5	20.014	3.185,3	0,00031394

PART 6

DISCUSSION AND CONCLUSION

This study has put forward by considering the gains to be achieved in terms of both mass and mechanical properties with the design for additive manufacturing of automotive components. One of the most preferred methods in DFAM is topology optimization. Thanks to this method, models can be designed lighter and more durable without being limited by manufacturing constraints.

This study focuses on the use of topology optimization in the design of automotive components for additive manufacturing. In the literature, it has been observed that the studies on topology optimization mostly deal with the subject alone. However, AM is an integral part for the production of optimized geometries with this method. In this study, AM and topology optimization are discussed together and the importance of harmony is emphasized.

Powder bed fusion, which is the most common metal additive manufacturing method, was used as the AM method, and the simp method, which is the most suitable for use with the finite element method, was used as the topology optimization method.

When the strength value is used as the goal and constraint in topology studies, displacement is used instead of stress. The reason for this is that the stress values during the topology study are higher than they should be due to the surface roughness and do not give objective results. Therefore, the stress value is only used to compare the first and last model.

Displacement values are considered to be slightly higher than those determined in the first geometry, especially in mass reduction strategies, so a preliminary idea is obtained about where material can be removed. Similarly, the natural frequency constraints are set a little higher. In this way, the upper limits of optimization were observed. The reason why natural frequencies are taken into account in optimization studies is to acquire a valid model in dynamic operating conditions.

In the case studies, the front lower control arm of the double wishbone suspension system, also called A-arm, was used. Structural analyses were performed with two different loading conditions for curb and gross weight. Topology studies were implemented in three different strategies: minimize the mass, minimize the maximum displacement and providing the best stiffness to weight ratio. The models obtained in 5 different topology optimization studies under 3 different strategies were evaluated with their variable analysis results. By using the models acquired as a result of the studies, the model ensuring the desired strength and mass values was obtained with the help of reverse engineering tools.

Fea was also performed on the model that emerged after the optimization and compared with the first results. In the first model, 70,51 MPa and 90,65 MPa von mises stress were measured for the curb and gross weight, respectively, while 69,01 MPa and 88,73 MPa were measured in the optimized model. While keeping the stress values at these levels, natural frequencies were kept within the desired range with the optimization constrains determined. The weight value was reduced from 10,80 kg to 9,03 kg, while the mechanical properties were kept almost constant. Thus, a %16,39 reduction was achieved.

REFERENCES

1. Mhapsekar, K., McConaha, M., and Anand, S., "Additive Manufacturing Constraints in Topology Optimization for Improved Manufacturability", ***Journal Of Manufacturing Science And Engineering***, 140 (5): (2018).
2. Reddy K, S. N., Maranan, V., Simpson, T. W., Palmer, T., and Dickman, C. J., "Application of topology optimization and design for additive manufacturing guidelines on an automotive component", ***International Design Engineering Technical Conferences And Computers And Information In Engineering Conference***, 50107: V02AT03A030 (2016).
3. Ranjan, R., Samant, R., and Anand, S., "Integration of design for manufacturing methods with topology optimization in additive manufacturing", ***Journal Of Manufacturing Science And Engineering***, 139 (6): (2017).
4. Tyflopoulos, E., Lien, M., and Steinert, M., "Optimization of brake calipers using topology optimization for additive manufacturing", ***Applied Sciences***, 11 (4): 1437 (2021).
5. Lian, H., Christiansen, A. N., Tortorelli, D. A., Sigmund, O., and Aage, N., "Combined shape and topology optimization for minimization of maximal von Mises stress", ***Structural And Multidisciplinary Optimization***, 55 (5): 1541–1557 (2017).
6. Lu, W., Xiao-kai, C., and Qing-hai, Z., "Muti-objective topology optimization of an electric vehicle's traction battery enclosure", ***Energy Procedia***, 88: 874–880 (2016).
7. Dalklint, A., Wallin, M., and Tortorelli, D. A., "Structural stability and artificial buckling modes in topology optimization", ***Structural And Multidisciplinary Optimization***, 64 (4): 1751–1763 (2021).
8. Kulkarni, V., Jadhav, A., and Basker, P., "Finite element analysis and topology optimization of lower arm of double wishbone suspension using Radioss and Optistruct", ***International Journal Of Science And Research***, 3 (5): 639–643 (2014).
9. Song, B. C., Park, Y. C., Kang, S. W., and Lee, K. H., "Structural optimization of an upper control arm, considering the strength", ***Proceedings Of The***

Institution Of Mechanical Engineers, Part D: Journal Of Automobile Engineering, 223 (6): 727–735 (2009).

10. Viqaruddin, M. and Reddy, D. R., "Structural optimization of control arm for weight reduction and improved performance", ***Materials Today: Proceedings***, 4 (8): 9230–9236 (2017).

11. Lin, Y. and Guo, S., "Study on Lightweight Optimization of Low Control Arm for Vehicle Suspension Based on Kinematic Envelope Analysis", ***Society Of Automotive Engineers (SAE)-China Congress***, 467–476 (2017).

12. Özarpa, C., Botsali, H., and Kinaci, B. F., "Raylı Sistemlerde Kullanılan Cer Kancasının Topoloji Optimizasyonuna Uygunluğunun Değerlendirilmesi", ***Demiryolu Mühendisliği***, (15): 1–12 (2022).

13. Guiggiani, M., "The Science of Vehicle Dynamics: Handling, Braking, and Ride of Road and Race Cars", ***Springer***, (2018).

14. Rill, G., "Road Vehicle Dynamics: Fundamentals and Modeling", ***Crc Press***, (2011).

15. Jazar, R. N., "Vehicle Dynamics: Theory and Application", ***Springer***, (2017).

16. Bastow, D., Howard, G., and Whitehead, J. P., "Car Suspension and Handling", ***SAE International Warrendale***, (2004).

17. Attaran, M., "The rise of 3-D printing: The advantages of additive manufacturing over traditional manufacturing", ***Business Horizons***, 60 (5): 677–688 (2017).

18. Saleh Alghamdi, S., John, S., Roy Choudhury, N., and Dutta, N. K., "Additive Manufacturing of Polymer Materials: Progress, Promise and Challenges", ***Polymers***, 13 (5): 753 (2021).

19. Wohlers, T. T., Associates (Firm), W., Campbell, I., Diegel, O., Huff, R., Kowen, J., and Mostow, N., "Wohlers Report 2021: 3D Printing and Additive Manufacturing Global State of the Industry", ***Wohlers Associates, Incorporated***, 374 (2021).

20. Brighenti, R., Cosma, M. P., Marsavina, L., Spagnoli, A., and Terzano, M., "Laser-based additively manufactured polymers: a review on processes and mechanical models", ***Journal Of Materials Science***, 1–38 (2020).

21. Gao, M., Li, L., Wang, Q., Ma, Z., Li, X., and Liu, Z., "Integration of Additive Manufacturing in Casting: Advances, Challenges, and Prospects",

International Journal Of Precision Engineering And Manufacturing-Green Technology, (2021).

22. Wohlers, T. T., Campbell, I., Diegel, O., Huff, R., and Kowen, J., "Wohlers Report 2020: 3D Printing and Additive Manufacturing Global State of the Industry", ***Wohlers Associates***, (2020).

23. Fotovvati, B., Balasubramanian, M., and Asadi, E., "Modeling and Optimization Approaches of Laser-Based Powder-Bed Fusion Process for Ti-6Al-4V Alloy", ***Coatings***, 10: 1104 (2020).

24. ISO/ASTM 52900: 2015 (E), "Standard terminology for additive manufacturing–general principles–terminology", (2015).

25. Sahini, D. K., Ghose, J., Jha, S. K., Behera, A., and Mandal, A., "Optimization and Simulation of Additive Manufacturing Processes: Challenges and Opportunities–A Review", Additive Manufacturing Applications for Metals and Composites, ***IGI Global***, 187–209 (2020).

26. Gu, D. D., Meiners, W., Wissenbach, K., and Poprawe, R., "Laser additive manufacturing of metallic components: materials, processes and mechanisms", ***International Materials Reviews***, 57 (3): 133–164 (2012).

27. Da Silva, L. R. R., Sales, W. F., Campos, F. dos A. R., De Sousa, J. A. G., Davis, R., Singh, A., Coelho, R. T., and Borgohain, B., "A comprehensive review on additive manufacturing of medical devices", ***Progress In Additive Manufacturing***, (2021).

28. Pratheesh Kumar, S., Elangovan, S., Mohanraj, R., and Ramakrishna, J. R., "Review on the evolution and technology of State-of-the-Art metal additive manufacturing processes", ***Materials Today: Proceedings***, (2021).

29. Sing, S. L., An, J., Yeong, W. Y., and Wiria, F., "Laser and electron-beam powder-bed additive manufacturing of metallic implants: A review on processes, materials and designs", ***Journal Of Orthopaedic Research : Official Publication Of The Orthopaedic Research Society***, 34: (2015).

30. Simchi, A., Petzoldt, F., and Pohl, H., "On the development of direct metal laser sintering for rapid tooling", ***Journal Of Materials Processing Technology***, 141 (3): 319–328 (2003).

31. Oinonen, O., "Utilization of laser-based powder bed fusion in manufacturing process of compression mold", (2020).

32. Bača, A., Konečná, R., Nicoletto, G., and Kunz, L., "Influence of build direction on the fatigue behaviour of Ti6Al4V alloy produced by direct metal laser sintering", ***Materials Today: Proceedings***, 3 (4): 921–924 (2016).

33. Wang, Y., Chen, X., Jayalakshmi, S., Singh, R. A., Sergey, K., and Gupta, M., "Process Parameters, Product Quality Monitoring, and Control of Powder Bed Fusion", Transactions on Intelligent Welding Manufacturing, ***Springer***, 89–108 (2020).

34. Urhal, P., Weightman, A., Diver, C., and Bartolo, P., "Robot assisted additive manufacturing: A review", ***Robotics And Computer-Integrated Manufacturing***, 59: 335–345 (2019).

35. Gu, D., "Laser Additive Manufacturing of High-Performance Materials", ***Springer***, (2015).

36. Liu, J., Gaynor, A. T., Chen, S., Kang, Z., Suresh, K., Takezawa, A., Li, L., Kato, J., Tang, J., Wang, C. C. L., Cheng, L., Liang, X., and To, Albert. C., "Current and future trends in topology optimization for additive manufacturing", ***Structural And Multidisciplinary Optimization***, 57 (6): 2457–2483 (2018).

37. Karayel, E. and Bozkurt, Y., "Additive manufacturing method and different welding applications", ***Journal Of Materials Research And Technology***, 9 (5): 11424–11438 (2020).

38. Zienkiewicz, O. C., Taylor, R. L., Nithiarasu, P., and Zhu, J. Z., "The Finite Element Method", ***McGraw-Hill London***, (1977).

39. Reddy, J. N., "Introduction to the Finite Element Method", ***McGraw-Hill Education***, (2019).

40. Segerlind, L. J. and Saunders, H., "Applied finite element analysis", (1987).

41. Internet: SOLIDWORKS, "Nonlinear Static Analysis Overview", **http://help.solidworks.com/2022/english/solidworks/cworks/c_nonlinear_static_analysis_overview.htm** (2022).

42. Hutton, D. V., "Fundamentals of Finite Element Analysis", ***McGraw-Hill***, (2004).

43. Vanam, B. C. L., Rajyalakshmi, M., and Inala, R., "Static analysis of an isotropic rectangular plate using finite element analysis (FEA)", ***Journal Of Mechanical Engineering Research***, 4 (4): 148–162 (2012).

44. Benzley, S. E., Perry, E., Merkley, K., Clark, B., and Sjaardama, G., "A comparison of all hexagonal and all tetrahedral finite element meshes for elastic and elasto-plastic analysis", ***Proceedings, 4th International Meshing Roundtable***, 17: 179–191 (1995).

45. Carrera, E., Cinefra, M., Petrolo, M., and Zappino, E., "Finite Element Analysis of Structures through Unified Formulation", ***John Wiley & Sons***, (2014).

46. Botkin, M. E. and Wang, H.-P., "An adaptive mesh refinement of quadrilateral finite element meshes based upon a posteriori error estimation of quantities of interest: linear static response", ***Engineering With Computers***, 20 (1): 31–37 (2004).

47. Hughes, T. J., "The Finite Element Method: Linear Static and Dynamic Finite Element Analysis", ***Courier Corporation***, (2012).

48. Internet: Autodesk, "Metrics and the Basics of Mechanics", **https://knowledge.autodesk.com/search-result/caas/simplecontent/content/metrics-and-the-basics-mechanics-part-2.html** (2022).

49. Meng, L., Zhang, W., Quan, D., Shi, G., Tang, L., Hou, Y., Breitkopf, P., Zhu, J., and Gao, T., "From Topology Optimization Design to Additive Manufacturing: Today's Success and Tomorrow's Roadmap", ***Archives Of Computational Methods In Engineering***, 27 (3): 805–830 (2020).

50. Zhu, J., Zhou, H., Wang, C., Zhou, L., Yuan, S., and Zhang, W., "A review of topology optimization for additive manufacturing: status and challenges", ***Chinese Journal Of Aeronautics***, (2020).

51. Reddy K, S. N., Ferguson, I., Frecker, M., Simpson, T. W., and Dickman, C. J., "Topology optimization software for additive manufacturing: A review of current capabilities and a real-world example", ***International Design Engineering Technical Conferences And Computers And Information In Engineering Conference***, 50107: V02AT03A029 (2016).

52. Wu, J., Sigmund, O., and Groen, J. P., "Topology optimization of multi-scale structures: a review", ***Structural And Multidisciplinary Optimization***, 63 (3): 1455–1480 (2021).

53. Zhan, T., "Progress on different topology optimization approaches and optimization for additive manufacturing: a review", ***Journal Of Physics: Conference Series***, 1939 (1): 012101 (2021).

54. Gao, J., Xiao, M., Zhang, Y., and Gao, L., "A Comprehensive Review of Isogeometric Topology Optimization: Methods, Applications and Prospects", ***Chinese Journal Of Mechanical Engineering***, 33 (1): 87 (2020).

55. Yunfei, B., Ming, C., and Yongyao, L., "Structural topology optimization for a robot upper arm based on SIMP method", Advances in Reconfigurable Mechanisms and Robots II, ***Springer***, 725–733 (2016).

56. Zhang, S., Li, H., and Huang, Y., "An improved multi-objective topology optimization model based on SIMP method for continuum structures including self-weight", ***Structural And Multidisciplinary Optimization***, 63 (1): 211–230 (2021).

57. Gebremedhen, H. S., Woldemicahel, D. E., and Hashim, F. M., "Three-dimensional stress-based topology optimization using SIMP method", ***International Journal For Simulation And Multidisciplinary Design Optimization***, 10: A1 (2019).

58. Internet: Paluneau, "Interpolation of Young's Modulus by the SIMP Method", **https://commons.wikimedia.org/wiki/File:Interpolation_du_module_de_Young_par_la_m%C3%A9thode_SIMP.svg** (2022).

59. Zuo, W. and Saitou, K., "Multi-material topology optimization using ordered SIMP interpolation", ***Structural And Multidisciplinary Optimization***, 55 (2): 477–491 (2017).

60. Ijagbemi, C. O., Oladapo, B. I., Campbell, H. M., and Ijagbemi, C. O., "Design and Simulation of Fatigue Analysis for a Vehicle Suspension System (VSS) and its Effect on Global Warming", ***Procedia Engineering***, 159: 124–132 (2016).

61. Singh, J. and Saha, S., "Static structural analysis of suspension arm using finite element method", ***International Journal Of Research In Engineering And Technology***, (2018).

62. Gadade, B. and Todkar, R. G., "Design, analysis of A-type front lower suspension arm in commercial vehicle", ***International Research Journal Of Engineering And Technology***, 2 (7): 759–766 (2015).

63. Internet: SOLIDWORKS Help-2022, "Analysis Solvers", **http://help.solidworks.com/2022/english/SolidWorks/cworks/c_analysis_solvers.htm?verRedirect=1** (2022).

RESUME

Hüseyin BOTSALI started undergraduate program in Gazi University Department of Manufacturing Engineering in 2011. In 2017, he started MSc. education in same place. From 2018 to 2021, he worked as a FEA expert at SOLIDWORKS distributer. Then in 2021, he has started assignment as a Research Assistant in Marmara University Department of Mechanical Engineering. He married in 2020 and he has a daughter. To complete M. Sc. education, he moved to Karabük University in 2020.